Accepted Manuscript

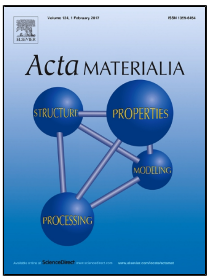

Influence of thermal properties and temperature of substrates on the quality of cold-sprayed deposits

Z. Arabgol, M. Villa Vidaller, H. Assadi, F. Gärtner, T. Klassen

PII:	S1359-6454(17)30052-6
DOI:	10.1016/j.actamat.2017.01.040
Reference:	AM 13502
To appear in:	*Acta Materialia*
Received Date:	21 September 2016
Revised Date:	17 January 2017
Accepted Date:	21 January 2017

Please cite this article as: Z. Arabgol, M. Villa Vidaller, H. Assadi, F. Gärtner, T. Klassen, Influence of thermal properties and temperature of substrates on the quality of cold-sprayed deposits, *Acta Materialia* (2017), doi: 10.1016/j.actamat.2017.01.040

Influence of thermal properties and temperature of substrates on the quality of cold-sprayed deposits

Z. Arabgol [a], M. Villa Vidaller [b], H. Assadi [c,*], F. Gärtner [b], T. Klassen [b]

[a] Tarbiat Modares University, Department of Materials Engineering, Tehran, Iran

[b] Helmut Schmidt University, Institute of Materials Technology, Hamburg, Germany

[c] Brunel University London, BCAST, Uxbridge, United Kingdom

Abstract

The properties of cold-sprayed deposits are often considered to depend mainly on the particle velocity and the particle temperature. The present paper demonstrates, through systematic experimentation and multi-scale modelling, that the substrate properties, too, influence the deposit properties, even in the regions far away from the substrate/deposit interface. Cold spraying experiments were performed with copper and titanium powders, using fixed process parameters, but different substrate materials and different substrate temperatures. As a measure of coating quality, the electrical conductivity of the coatings was evaluated on the top surface of (0.8-1 mm) thick coatings. The coating conductivity was found to depend strongly on the initial temperature and the thermal effusivity of the substrate. The mechanical properties of the substrate, also, influence the local coating properties, but only in the regions within 50 μm distance from the substrate/coating interface. The temperature and the thermal effusivity of the substrate control the instantaneous temperature of the top surface layer of the already deposited material, thus influencing the extent of particle bonding and the coating properties. These findings underline the role of thermal management in cold spraying.

Keywords: Cold spray, Substrate effect, Modelling, Particle impact, Heat transfer.

* Corresponding author, e-mail: hamid.assadi@brunel.ac.uk

1. Introduction

Cold spraying is a solid-state coating process, in which material deposition takes place by high-velocity impact, severe deformation, and bonding of microparticles [1]. Like explosive welding, deformation in cold spraying is associated with adiabatic shear instability (ASI) and large plastic deformation at the contact area [2-5]. The critical velocity of bonding – i.e. the minimum particle impact velocity required to create bonding – depends on various factors, most importantly on the temperature and the thermomechanical properties of the respective particle and substrate materials [2, 6]. The main coating properties have been shown to be a unique function of the ratio of particle velocity to critical velocity, here referred to as η [7]. Many previous studies have aimed to understand bonding mechanism, to evaluate the critical velocity, and hence η, for different materials and process conditions [4, 7-18]. So far, none of the suggested formulae for the critical velocity and η incorporate substrate properties.

In cold spray deposition, there are two distinct types of interaction that should be distinguished from one another: (i) particle-to-substrate interaction, which is necessary for the formation of the first layer of particles, being relevant for the adhesive strength of the final coating on the substrate, and (ii) particle-to-particle interaction, which concerns the build-up of the coating, and relates to the cohesive strength of the deposit [19, 20]. This means that the critical velocity for the deposition of the first layer of particles may be different from that of the next layers, particularly for the case of dissimilar coating and substrate materials [20-22]. For dissimilar materials, therefore, the cohesive strength of a cold-sprayed deposit may be rather different from the (adhesive) bond strength between the coating and the substrate. While the latter can be influenced significantly by the substrate material, temperature and surface conditions, the former might seem to be independent of the substrate-related factors [3, 8, 15, 19-30]. This is in fact not true. As will be discussed later, there are indications of the influence of substrate type and conditions not only on the adhesive strength, but also on the

cohesive strength, electrical conductivity, and the related 'bulk' properties of the cold-sprayed deposits, even at regions far (hundreds of microns) away from the substrate/coating interface [20, 22, 23, 29, 31, 32]. This might seem somewhat surprising, because the coating properties – such as the cohesive strength – are conceived to be influenced by the second type of bonding (particle-to-particle) as explained above. In other words, it is not clear how the substrate conditions can influence particle-to-particle bonding within the coating, particularly in regions that are 'isolated' from the substrate by several layers of the already deposited material.

Despite indications of strong substrate effects, most cold spray studies have focused on the effect of process parameters – such as gas pressure and temperature – on coating characteristics [17, 33-38]. Also, much attention has been paid to the formation of the first layer, and hence, on the adhesion of the coating to the substrate. For instance, it has been shown how the hardness and temperature of the substrate may influence the adhesion strength [19-32, 39, 40]. The effect of substrate hardness on adhesion strength may be interpreted in view of particle-substrate interaction – type (i) as mentioned above. Harder substrates make impacting particles deform more severely, whereas softer substrates result in smaller deceleration and hence less severe particle deformation [8, 19-23, 41]. On the other hand, softer substrates deform more severely under particle impact, which could result in ASI on the substrate side and hence promote bonding. For cold spraying of copper, for instance, the value of bond strength for aluminium and copper substrates are about four times higher than that for the low carbon steel substrates [42]. It is also shown that substrate preheating generally increases the adhesion strength and the deposition efficiency of the first layers [25-27, 29, 39].

Examples of studies that indicate the effect of substrate material on the coating properties are given in Refs [20, 22, 23, 29, 31, 38]. (Note that the coating properties concern type (ii) interaction as mentioned above.) For example, tensile strength of cold-sprayed titanium

coatings was shown to be 20 % higher for 304 stainless steel (EN 1.4301) substrates as compared to AlMg3 substrates [38]. Moreover, the strength of copper coatings nearly doubled when cold spraying was on steel substrates as compared to when it was on copper substrates [29]. There are also numerical investigations with different combination of materials, showing that substrate hardness may affect coating performance, but this was demonstrated only for a case where the coating was relatively thin [41]. Several investigations [25, 31, 32, 39] suggest that substrate temperature can influence the deposition efficiency, e.g. in bulk metallic glasses. Improved coating properties – strength, cavitation resistance or conductivity – could be obtained by substrate preheating in cold spraying of copper [29] and bronzes [43]. Conversely, there have also been studies that show no obvious effect of the substrate temperature on the coating porosity, microstructure, or hardness, e.g. in cold spraying of copper and aluminium [26, 44]. This discrepancy could have resulted from differences in the employed method of substrate heating in different studies. In one group of experiments, low power heaters are used, so that the substrate temperature is initially high but it is substantially reduced because of cooling by the gas stream during the spray process [31, 44]. In another group of experiments, high power controls are used, which guarantee constant substrate temperature throughout the whole process duration [29, 43]. In any case, whether or in what sense the substrate temperature affects the coating quality has remained an open question.

It should also be noted that substrate hardness decreases with increasing temperature. Therefore, it may seem that substrate preheating affects coating properties merely via thermal softening of the substrate. It is nevertheless not clear how a change in the mechanical property of the substrate can influence type (ii) interactions, especially in regions far away from the substrate. In summary, the influences of the type of substrate material and the substrate temperature on coating properties call for further investigations. The present work aims to

provide such a basis by combining systematic experimentation with modelling at different length scales. With this aim, the present work focuses on the following specific questions:

1. Does the substrate effect – on type (ii) interactions – exist? In other words, is there an influence of the substrate conditions – such as dimensions, material properties and the initial temperature – not only on the adhesive strength, but also on the properties of cold-sprayed deposits? If so, what are the influential factors and how do they influence these properties?

2. Where does the substrate effect, if present, originate from? How can the substrate 'communicate' its properties to the deposited material in locations far away from the coating/substrate interface? What substrate properties, i.e. mechanical or thermal, are more relevant? How can the substrate effect be predicted and controlled?

To answer the first set of questions, a series of experiments have been designed and carried out, in which properties such as the hardness and electrical conductivity of the cold-sprayed coatings have been evaluated for the same spraying conditions, but different substrate materials and initial temperatures. For this purpose, the ultimate tensile strength (UTS) as obtained using the micro flat tensile (MFT) test may be a considered to be a most suitable property. The MFT test result is a reliable measure of the coating quality, e.g. as demonstrated for copper coatings [6, 45]. However, MFT test is restricted to relatively thick coatings and is therefore not always straightforward to implement. Alternatively, the electrical conductivity of a coating may be used to obtain information on the coating quality, as well as on the level of defects and impurities such as oxygen or nitrogen [29, 46]. The measurement of electrical conductivity, using the eddy current method, is based on the analysis of electron mobility in plane of the coating layers. For cold sprayed titanium coatings [47], a strong correlation exists between the electrical conductivity and the UTS, as obtained using the MFT test, Fig. 1. Both quantities are highly anisotropic, but in this case, they correspond to the same (in-plane) direction. In view of the above correlation, the electrical conductivity is used in the present

study as a convenient measure of the coating quality, and so, of the extent of bonding between adjacent particles within the coating [32, 46, 48] – pertaining to type (ii) interactions.

Modelling and simulation of the relevant thermomechanical processes in cold spraying have been pursued to provide an insight to the second set of questions, as mentioned above. A main objective of the theoretical analysis is to work out the extent of bonding between neighbouring particles within the coating, which could be compared with the measured electrical conductivities. Furthermore, modelling is used to investigate the influence of process parameters and substrate properties on the fraction of bonded area. Specifically, two different sets of substrate properties are considered and studied separately: (a) the mechanical properties, and (b) the thermal properties. In this way, the relevant substrate parameters are identified in view of the experimental results.

2. Methods

2.1. Experiments

Cold spraying

Commercial purity (CP) grade 2 (≥ 99.92 wt.%) titanium powder from AP&C Raymor Industries Inc., (Boisbriand, Canada) and OFHC copper powder from TLS Technik GmbH & Co. Spezialpulver KG (Bitterfeld, Germany) were used as feedstock for the experiments. The particles of the titanium powder – prepared by plasma wire spraying under argon atmosphere – were spherical and without porosity, Fig. 2. The size distribution of the titanium powder was as follows: d_{10} = 15 µm, d_{50} = 34 µm, d_{90} = 59 µm. The copper powder used in the experiments was produced by inert gas-atomization in nitrogen atmosphere with 99.95 wt. % Cu purity. The particles of the copper powder were also spherical and without porosity, but unlike the titanium powder, contained some fine satellites, Fig. 3. The amount of satellites did

not appear to be critical for causing nozzle clogging by in-flight separation. The size distribution of the copper powder was as follows: d_{10} = 25 µm, d_{50} = 41 µm, d_{90} = 66 µm.

The spray process was performed by using the Helmut-Schmidt-University prototype of the Kinetiks 8000 system, later launched to the market by CGT (Ampfing, Germany). Modifications as compared to the commercial system concern a higher nominal heating power of 92 kW, and a longer pre-chamber allowing for sufficient preheating of coarser powders [47, 49, 50]. Nitrogen was used as process gas, and spraying was performed with a water-cooled WC-Co nozzle (type 24). The spraying distance was set to 60 mm and the line spacing to 2 mm. The powder feed rate was 9.4 cm^3/min, and the spraying gun traverse speed was set to 235 mm/s. The point of powder injection was set to 180 mm upstream the nozzle throat to ensure sufficient preheating of all particle sizes to the temperature of the process gas. The coatings of CP titanium were applied onto 3 mm thick titanium and copper plates and 4 mm thick steel 1.4301 substrates with the lateral dimensions of 70 mm ×70 mm. The OFHC copper was sprayed onto substrates of copper, 3 mm in thickness, as well as onto 4-mm thick AlMg3 and Al-7075-T6 substrates. Substrate heating was performed by using a specially-designed 15 kW induction heater, positioned at the back of the substrate holder. To control the temperature, a thermocouple was mounted into the substrate just 1 mm below the surface, using a side bore of 15 mm depth –i.e. sufficiently deep to avoid convection effects. The induction heating provided high power and fast response to minimize temperature variations cause by the process gas and the ambient air stream, as well as by building up coatings over several spray layers [29].

The spraying parameters (temperature and pressure) were selected – by using the commercial software package KSS from Kinetic Spray Solutions (Buchholz, Germany) – to obtain a velocity ratio ($\eta = v_p / v_{crit}$) of slightly above unity. The calculated particle velocities was cross checked by velocity measurements using a ColdSpray meter from Tecnar (Saint-Bruno-de-

Montarville, Canada) and alumina as spay powder to ensure higher data yield. The selection of marginally low spraying conditions was to assure deliberately poor coating qualities, and thus, to increase the sensitivity of the results to any possible substrate effects. Cold spraying of titanium was performed at a process gas pressure of 40 bar and process gas temperatures of 600 °C and 800 °C, corresponding to η values of 1.00 and 1.16, respectively. For cold spraying of copper, a process gas pressure of 30 bar and a process gas temperature of 320°C were chosen, corresponding to an η value of 1.17.

Electrical conductivity measurement

An eddy current method using a Sigma Scope smp 10 from Helmut Fischer GmbH (Sindelfingen, Germany) was used to measure the electrical conductivity. To reach low penetration depths of about 500 µm, a frequency of 1250 kHz was used. 10 individual measurements were carried out on both the as-sprayed and then polished surfaces of the coatings.

Hardness testing

The hardness testing was used as a complementary characterisation method, in addition to electrical conductivity measurements. The hardness was measured with a micro hardness tester Miniload II from the company Leitz, Wetzlar, Germany. The instrument measures the hardness in Vickers according to the specifications of ASTM E384-10. The hardness was determined as HV 0.3 with a test load of 2,942 N on the cross sections.

2.2. Modelling

Modelling and simulation of cold spray deposition was carried out at two different length scales as follows: (a) micro-model of particle impact – with the objective of estimating the fraction of highly-strained area (HAS) in the corresponding contact surfaces, for various

substrate properties and coating thicknesses; (b) macro-model of heat transfer – with the objective of calculating the temperature of the top layer of the coating upon particle impact. The results of the macro-model are subsequently fed into the micro-model, namely to investigate the effect of the surface temperature of the substrate/coating on the respective HSA fraction. Figure 4 shows the modelling setup used in this study. The numerical results are further discussed in view of an analytical model of heat transfer. The modelling methods are described in more detail below.

Particle impact

To investigate the effect of substrate material and temperature on the fraction of bonded area, as a general measure of coating quality, particle impact was simulated through an axisymmetric model using the finite-element software Abaqus/Explicit. A coupled temperature-displacement analysis was used to account for the thermomechanical response of materials under high strain-rate deformation and transient heat transfer conditions. Initially, the impact was assumed to be on a substrate with a pre-deposited coating layer. The particle diameter was 50 μm (corresponding to the larger particles of the powders used in the experiments). The thickness of the pre-deposited coating was varied from 5 to 300 μm, to investigate the sole effect of substrate hardness on particle-particle bonding, as a function of coating thickness. Two sets of simulations were performed for copper and titanium particles. Aluminium and steel were selected as substrate materials for copper coatings. For the case of titanium, the substrate material was assumed to be titanium. For all cases, the Johnson-Cook model was employed to describe the rate and temperature dependence of material plasticity. Table 1 gives the material parameters, taken from literature [2, 8, 20, 51, 52].

The contact area between the particle and the deposited layer is usually considered to be bonded in the regions where there is an indication of adiabatic shear instability (ASI) on the surface of particle or substrate. This is usually associated with the emergence of relatively

large plastic strains of about 10 [53]. Simulation of such large strains and direct diagnosis of ASI are nevertheless not straightforward, mainly due to the numerical problems associated with excessive mesh distortion. As a workaround, ASI can be indirectly diagnosed by considering smaller thresholds of plastic strain, e.g. 2-3 on compromised mesh sizes [2, 4, 5]. In the present study, the extent of bonding is taken to correlate with the surface area of the interfacial region with an equivalent plastic strain (PEEQ) beyond 2 – here referred to as the "highly-strained" area (HSA). The fraction of HSA with respect to the overall contact area is thus taken to represent indirectly the extent of shear instability and bonding. It should be noted that the HSA fraction as defined here does not scale linearly with the fraction bonded. For the current model settings, HSA fractions of 0.7 and 0.8 correspond roughly to bonded fractions of 0.1 and 0.4, respectively.

The particle impact velocity was set to 450 m/s in the models with copper particles, and 650 m/s for those with titanium particles. These velocities were chosen in accordance with the critical conditions for bonding as calculated by the KSS software. The particle impact temperatures for copper and titanium were 25 °C and 400 °C, respectively. These velocities are only slightly greater than the critical velocity of the respective material – i.e. about 15 %, corresponding to $\eta = 1.15$. For both cases of copper and titanium particles, various surface temperatures in the range 25-1000 °C were considered for the impact simulations.

Macro-modelling of heat transfer

During the cold spraying process, there is a heat flux from the impinging gas and particles on the substrate/coating, resulting in a transient increase of the coating surface temperature. There have been studies using advanced modelling of heat transfer from the cold spray gun to the substrate [54-59]. These studies are based on computational fluid dynamics (CFD) and provide an accurate account of the temporal evolution of the temperature field within various substrates. For the present study, we used a simple heat transfer model to estimate the

maximum surface temperature, i.e. the temperature of the substrate/coating upon particle impact, for titanium and copper coatings. This temperature, in addition to the particle impact temperature, is conceived to play an important role in particle bonding [39, 60]. The model consists of a holder, a substrate, and a pre-deposited coating layer. The heat input is applied by considering convective heat transfer (film condition in Abaqus) on the top layer of the coating, like the method as described in a previous work [61]. The thickness of the substrate holder and the substrate are both assumed to be 3 mm. The coatings are assumed to be 1 mm thick. Three different substrate materials (copper, titanium, and stainless steel) at three different temperatures (27, 200 and 400 °C) were considered, consistent with the current experiments on cold spraying of titanium. The coating surface temperatures obtained from the macro-model are subsequently used as the substrate/coating temperature in the impact model, to investigate the effect of temperature on the fraction of highly strained area (HSA). The thermal properties of coatings are taken the same as those of bulk material, as a first approximation.

Analytical model of heat transfer

Further to numerical modelling, a simple analytical model of heat transfer is developed to relate the coating surface temperature to the thermal properties of the substrate. The reason for developing an analytical model is to fit the numerical results, and by doing so, to demonstrate that 'effusivity' is the most relevant thermal property of the substrate in cold spraying. The thermal effusivity is a measure of the ability of a material to exchange thermal energy with its surroundings, defined as:

$$e = \sqrt{k\rho c_p} \tag{1}$$

where k is the thermal conductivity, ρ is the density and c_p is the specific heat. The values of thermal effusivity of different substrate materials as considered in this study are given in table

1. The analytical model is based on a few crude assumptions as follows. The substrate dimensions (70 mm) are assumed to be significantly larger that the spraying spot size (8 mm) so that a semi-infinite model of heat transfer is considered. Moreover, the thermal effusivity of the coating/substrate assembly is taken to be the weighted average of those of the coating and the substrate:

$$e = fe_{\text{substrate}} + (1-f)e_{\text{coating}} \tag{2}$$

where f is the weighting factor. On the other hand, the thermal interaction between the gas stream and the substrate is taken to be governed by convection. For a semi-infinite body with a constant surface temperature, the heat flux is given as:

$$q_c = \frac{k(T_i - T_0)}{\sqrt{\pi\alpha t}} = \frac{e(T_i - T_0)}{\sqrt{\pi t}} \tag{3}$$

where e is the thermal effusivity, T_i is the surface temperature, and T_0 is the initial temperature. Assuming convection at the surface, the convective heat flux may be written as:

$$q_h = h(T_g^* - T_i) \tag{4}$$

where h is a time-dependent heat transfer coefficient, and T_g^* is the 'effective' gas temperature. Equating (1) and (3) gives the surface temperature:

$$T_i = T_0 + (T_g^* - T_0)\frac{\bar{h}}{\bar{h} + e} \tag{5}$$

where $\bar{h} = h\sqrt{\pi t}$ is a 'constant' with the dimension of effusivity. By taking both $\bar{h}$ and T_g^* as adjustable parameters, Eq. (5) is used as a fitting function to adjust the results of the numerical macro-model. As mentioned above, this is a crude fitting function, because the substrate is not in fact semi-infinite, and the surface temperature is a time-dependent variable.

3. Results

3.1. Experimental evidence for the effect substrate on coating properties

During cold spraying, the initial substrate temperatures due to heat exchange with the process gas showed some changes. Starting at room temperature, the recorded substrate temperature increased up to about 70 ± 20 °C during the deposition of up to 4 spray layers. The initial temperatures of 200 °C kept rather constant during spraying within a range of ± 30 °C. Using higher initial temperatures of 350 and 400 °C, a decrease of about 50°C was observed after the first spray pass, then remained constant at 300 and 350° ± 20 C, respectively. Note that the temperature gradient from the surface to the position of the thermocouple varies during the multi-pass cold spraying, so that the surface temperature may not remain constant even for constant thermocouple recording. The macro model complements the measurements to provide a more precise description of the effective surface temperature.

Figure 5 shows examples of the cross-section of copper and titanium coatings obtained on different substrates at room temperature. Due to relatively low values of η (1.1 to 1.2) the coatings show noticeable levels of porosity (up to 5 %) – as expected. Within the examined range of parameters, no obvious influence of the substrate material or temperature on the porosity was observed. The cold sprayed copper coatings on copper, AlMg3 and Al 7075 show roughly the same thickness, indicating similar deposition efficiencies, despite differences in hardness and density of the substrates. For cold spraying titanium, on the other hand, small differences in coating thickness were observed; slightly higher for the titanium than for the copper and steel substrates. The observed differences in thickness, or deposition efficiency, did not show any correlation to the substrate strength or density.

Figure 6 shows the variation of the coating hardness with the substrate temperature for different substrate materials. For the copper coatings on copper, AlMg3 and Al 7075

substrates, the hardness decreases from about 130 HV 0.3 to about half of this value with increasing substrate temperatures to 350 °C. The substrate material, on the other hand, does not seem to play a role in the observed trend. For cold spraying titanium onto the different substrate materials examined in this study, the coating hardness does not noticeably change. Only for the steel substrate, there is a weak trend indicating an influence of substrate temperature on the coating hardness.

The measured electrical conductivities of the top layer of the obtained copper and titanium coatings are shown in Figure 7. The standard deviations of the individual values are in the range of 0.2 to 0.6 % of the absolute values of the measured electrical conductivities. For all cases of cold sprayed copper and titanium coatings, the electrical conductivity increases with increasing the initial temperature of the substrates. Increasing the initial substrate temperature from 20 °C to 350 °C increases the conductivity of copper coatings by about 20 %. For these coatings, the measured conductivity is almost independent of the selected substrate material. For titanium coatings, on the other hand, the substrate material has a prominent effect on conductivity. On the steel or titanium substrates at room temperature, titanium coatings exhibit similar and relatively high conductivities. For these substrates, rising the initial temperature to 200 °C does not lead to substantial changes in conductivity. A further increase of substrate temperature to 400 °C results in an about 8 % increase in conductivity. In contrast, coatings on copper substrates show (about 10 %) lower conductivities for all the different initial substrate temperatures.

3.2. Impact simulations

Figure 8 shows snapshots of simulated impacts of copper particles on hard (steel) and soft (aluminium) substrates, for different thicknesses of the pre-deposited coating layer. For the thinnest layer, i.e. 5-µm thick, the difference between the two cases of soft and hard substrates is most significant. For the coating thickness of 5 µm, the particle is markedly flattened on the

steel substrate, while the substrate is barely deformed. Significant flattening of the particle in this case results from severe deceleration of the particle. This is because a hard substrate constrains deformation of a thin interlayer. In contrast, the aluminium substrate is significantly deformed in the case of 5-µm thick coating. Thus, the deformation of the interlayer is not severely constrained, and the particle is not as much flattened than for cases impacting on a hard substrate. As shown in the figure, the effect of the substrate in constraining the deformation of the coating layer becomes less significant with increasing its thickness. This effect is shown more quantitatively in Fig. 9. The profiles of plastic strains on a meridian path over the particle surface for the two cases of hard and soft substrates become more similar with increasing the layer thickness. This implies that the mechanical properties of the substrate have a significant influence on the particle deformation only when the coating is relatively thin. Figure 9 also shows that the width of the highly-deformed regions – showing strains of above 2 – varies with the coating thickness. The trend of this variation depends on the substrate material.

The extent of highly deformed regions at the interface (the HSA fraction) monotonically correlates with – and is hence taken to represent – the extent of shear instability. It should be noted here that the amount of highly strained area or ASI at the particle surface may not necessarily be taken as a direct measure of bonding. Ideal bonding requires similar deformation of the underlying layer and the particle to ensure intimate contact. Thus, the amount of HSA is only to provide qualitative information on the effect of substrate properties on the extent of bonding.

Following the procedure described above, the fraction of highly-strained area (HSA) on the particle surface can be derived from the plastic strain profiles (Fig. 9) as a function of the interlayer thickness. Respective results are summarised in Fig. 10. It is interesting to note that the two substrate materials show different trends: for the harder (steel) substrate, the HSA

fraction on particle sites decreases with increasing the coating thickness, while this is the opposite for the softer (aluminium) substrate. Recording the deformation at interlayer surfaces would show opposite trends (not shown here), with high amounts of HSS using soft aluminium substrates decreasing with interlayer thickness, and low amounts of HSA on hard steel substrates showing an increase. Nevertheless, the values of HSA fraction for both substrate materials become comparable at a coating thickness of about 25 µm, almost identical at 50 µm, and remain unchanged for larger coating thicknesses. This demonstrates that the purely mechanical effect of the substrate on the coating properties – i.e. those related to particle deformation and HSA fraction – is only significant below 50 µm coating thickness. Beyond 50 µm, the mechanical properties of the substrate can hardly be 'communicated' through the deposited layers. In other words, particle deformation becomes insensitive to the hardness of substrate beyond a certain coating thickness. This finding agrees with the previous observations, e.g. in Ref [41].

It should be noted that in the modelling of particle impact, the temperature of the coating/substrate assembly represents the instantaneous temperature of the top layer of the coating upon particle impact. This is referred to as the 'coating surface temperature' in the subsequent macro modelling of heat transfer. As will be shown below, the coating surface temperature depends on different factors, such as the initial substrate temperature and the substrate thermal properties. Also, note that in the modelling of particle impact the coating is assumed to be 300 µm thick, as to evade any mechanical influence of the substrate.

Figure 11 shows the results particle impact simulations for cold spraying of titanium onto titanium, where the coating surface temperature is varied. Within the experimentally relevant range of surface temperature, the HSA fraction on the particle side slightly decreases with increasing the coating surface temperature up to 600°C, followed by slight increase. On the other hand, there is a significant increase in the HSA fraction on the substrate side with

increasing temperature. This results in an increase of the overall, here the mean HSA fraction – considering both substrate and particle – with increasing the surface temperature. In view of these results, the surface temperature appears to have a positive effect on the coating quality at fixed spraying conditions. That is, the higher is the coating surface temperature, the higher will be the mean HSA fraction, and the more favourable the coating properties.

3.3. Heat transfer modelling – coating surface temperature

The main objective of the heat transfer modelling is to work out the coatings surface temperature – which is found to be a most determining factor influencing coating properties – as a function of spraying parameters and substrate properties (material, thickness, and initial temperature). The overall results of heat transfer modelling for the case of titanium coatings are shown in Fig. 12. The calculated effective surface temperatures show a linear correlation with the initial substrate temperatures, but with different slopes. The coating surface temperatures are expectedly higher for titanium or steel substrates than for copper substrates. Moreover, the figure reveals that (i) the coating surface temperatures are significantly higher than the initial substrate temperatures and that (ii) the difference between the surface and initial substrate temperatures decreases with increasing the preheating. The former indicates a severe influence by heating through the gas jet, which is consistent with previous studies using advanced modelling of heat transfer [54-59].

The fitting parameters f, $\bar{h}$ and T_g^* in equations (2) and (5) are chosen respectively as 0.12, 25 kJ/m^2/K/s$^{1/2}$ and 570 °C, to give the best fit for the cases with titanium substrate. Interestingly, the same fitting parameters result in an equally good fit for the cases with copper substrate. For the cases with steel substrate, too, a reasonably good fit is obtained. The FEM simulations assume the so-called film condition (convective heat transfer). This is a crude simplification, but serves the purpose of this paper, which is to demonstrate the general

trends of variation of the cold-sprayed deposit properties as a function of the substrate properties. The heat transfer coefficient has been assumed to be 17 kJ/m^2/K. The results of both numerical and analytical models indicate an increase of coating surface temperature with increasing the initial substrate temperature. They also show that substrate materials with higher thermal effusivity result in lower surface temperatures. As indicated in table 1, thermal effusivity of steel and titanium are comparable, while the effusivity of copper is about five times higher. In reality, the surface temperature may be influenced by several other factors, which are not considered in the present study. For instance, a faster gun traverse speed, a larger standoff distance, a lower process gas temperature, a thicker substrate, or substrate cooling lead to a decreased surface temperature, and hence, to a decreased HSA fraction.

4. Discussion

4.1. Effect of substrate on hardness

The observed decline of hardness at higher substrate temperatures for the cold sprayed copper coatings could be attributed to thermal recrystallization. As reported by Ernst *et al.* [29], cold spraying of copper onto preheated substrates results in coating properties that are like those obtained by post annealing treatments. In cold spraying, recrystallization takes place during cooling down to room temperature. Borchers *et al.* [62] demonstrated thermal recrystallization at some (presumably highly deformed) regions within cold sprayed copper coatings, even when the substrate was not preheated. For the titanium coatings in this study, variations in coating hardness are less prominent, presumably due to only partial or negligible recrystallization. As a rough estimate, thermal recrystallization in titanium should occur just above 500°C, i.e. 0.4 times the melting temperature. Deformation at temperatures of up to 450°C causes merely dynamic recovery of CP titanium [63]. On the other hand, thermal recrystallization of highly cold-worked CP-titanium is expected to occur at temperatures well

above 500°C [64]. The coating and surface temperatures are below these characteristic temperatures.

Coating hardness is influenced by counteracting phenomena, i.e. it is increased by strain hardening and reduced by porosity, recovery and recrystallization. The cold-sprayed deposits have a very inhomogeneous microstructure, which could incorporate all of these factors at the same time, though in different proportions. The inhomogeneity in microstructure might be considered in analogy with a dual-phase or composite material. For metal-ceramic composites, the hardness increases almost linearly with the amount of hard-phase [65]. Likewise, the coating hardness would be expected to decrease with increasing porosity and to increase with increasing the amount of locally strain-hardened areas [54]. Considering only the effect of inhomogeneous strain hardening might cause a slight increase in hardness for higher surface temperatures. At lower surface temperatures, plastic work would be confined mainly to the impacting particle, which is typically hotter and hence more deformable than the already adhering spray layer. By increasing the substrate or surface temperature, the deformation region extends further into the deposited layer. Thus, the overall volume fraction of the strain hardened material, hence the overall hardness, may increase by increasing substrate and thus surface temperature. This effect may nevertheless be counteracted by recovery and recrystallization. Thermal recrystallization has been observed in cold spraying, even for titanium – with a relatively high recrystallization temperature of about 500°C– as sprayed onto substrates at room temperature [66]. The resultant softening depends largely on the extent of thermal recrystallization within the material. The recrystallization extent depends, on the one hand, on the local amount of plastic strain – hence on the driving forces for recrystallization – and, on the other hand, on the local thermal history. This means that recrystallization effects would presumably be more prominent for substrate materials of lower thermal effusivity, allowing for higher surface temperatures under the spray spot.

4.2. Effect of substrate on electrical conductivity

The electrical conductivity of cold sprayed coatings correlates with the cohesive strength of the coating and can be used as a measure of coating quality, representing the fraction of well-bonded interface [32, 45, 47]. It should be noted that the electrical conductivity may also be influenced by a variety of other factors – such as dislocation density and other structural defects – as brought about by high-velocity particle impact. Nevertheless, the effect of structural defects should in principle be separable from that of the 'fraction bonded' (here assumed to correlate with the HSA fraction) for the following reasons. First, the increase of defect density and the increasing of fraction bonded influence electrical conductivity in opposing ways. Second, both defect density and fraction bonded increase with increasing the impact velocity. Therefore, by increasing the particle impact velocity, the electrical conductivity should on the one hand improve because of a larger fraction bonded, and on the other hand, degrade because of larger defect density. This means that an improved electrical conductivity – for a more-or-less fixed porosity as observed in the present study – should have inevitably resulted from a larger fraction bonded, and vice versa. An exception to this rule is when there is an additional effect from recovery or recrystallization. In such a case, an increase of electrical conductivity with increasing substrate preheating temperature can be attributed to better particle bonding and, and also, to a smaller number of defects. It should be noted here that the strain distribution in cold sprayed coatings is rather inhomogeneous, resulting in a range of locally different recrystallization temperatures [42]. Thus, the reduction of hardness of cold sprayed copper coatings stretches over an annealing temperature regime of 200-400 °C.

For copper coatings, therefore, the marked change in conductivity with increasing substrate temperature may be attributed mainly to recrystallization. This interpretation is consistent with the hardness measurements, which show a decrease in hardness with increasing substrate

temperature. For titanium coatings, in contrast, the hardness shows only small changes, suggesting a lesser role for recrystallization. In this case, the change in fraction bonded could be taken as the main reason for the change in conductivity. Thus, the increase in conductivity for higher effective surface temperatures can be attributed to improved coating quality.

4.3. Experiments vs. modelling

For the case of titanium coatings, there is a remarkable similarity between the trends shown in Fig. 7b (experiments) and Fig. 12 (modelling). Assuming that the electrical conductivity correlates with the fraction bonded, and that they both represent the coating quality, the experimental results seem to be in reasonably good agreement with the modelling predictions. Note that this consistence is achieved by considering the thermal effects only. In both cases, the measured and the modelled 'coating quality' improves with increasing the initial substrate temperature. Moreover, there is a wide gap between the coating qualities for the substrates with a large difference in their thermal effusivity; spraying onto copper substrates results in a significantly lower coating quality than spraying onto steel substrates. For the copper coatings (Fig. 7a) the results are almost the same for the different substrate materials, which have comparable thermal effusivities. Thus, the substrate effect in regions far away from the coating/substrate interface seems to be mainly thermal in nature, and attributed to differences in effective surface temperatures. It should be noted that these thermal effects may involve recrystallization, which is not considered in the present analysis.

Fig. 13 shows the measured electrical conductivities as a function of the (temperature-dependent) tensile strength of the substrate (a) and the calculated coating surface temperature (b). This is done for all substrate conditions, i.e. the different substrate materials and initial substrate temperatures.

The experimental conductivity data in Fig. 13a and 13b are the same; the only difference concerns the variable on the x-axis, which is substrate strength in (a) and surface temperature in (b). Fig. 13a shows no direct correlation to the substrate strength, although there is a systematic increase of conductivity with decreasing substrate strength for individual substrate materials. Nevertheless, the plot demonstrates that there is no universal dependence of coating properties on the substrate strength.

In contrast, the measured thermal conductivities appear to correlate well with the coating surface temperature, Fig. 13b. The slight scatter can be attributed to uncertainties in coating thickness and in surface temperature calculations. Overall, the rather high coefficient of determination demonstrates that the deposit properties are greatly influenced by the thermal conditions of the substrate.

Figure 13 reconfirms that if there is any influence from the substrate on the quality of coating in regions far away from the coating/substrate interface, then it is most probably a purely thermal effect. The results also show that the temperature of the top layer of the coating upon particle impact is a most relevant factor in cold spraying. The surface temperature governs the overall deformability of the substrate. Therefore, not considering the detrimental effect of possible oxide layers, the bonded area is generally expected to extend at higher substrate temperatures. This finding agrees with the previous studies indicating higher coating qualities to be expected at higher substrate temperatures, either directly by substrate preheating [25, 27, 29, 31, 39] or indirectly by reducing the traverse gun speeds [67, 68].

5. Conclusions

Cold spray experiments where performed with different substrate materials at different initial temperatures, to study the effect of substrate conditions on the properties of cold-sprayed deposits. The results showed that the substrate condition does indeed have an influence on the

properties of cold-sprayed coatings, even at layers far (up to a millimetre) away from the substrate/coating interface. In combination with multiscale modelling of cold spray deposition, it is demonstrated that this effect can be attributed mainly to the thermal effusivity of the substrate. The mechanical properties of the substrate, in contrast, may affect the coating properties only within a limited range of coating thickness (typically less than 50 μm). In view of these findings, the coating surface temperature upon particle impact was identified as a most determining factor in coating quality. Particle impact simulations showed that the fraction of highly strained area (correlating with the fraction bonded) increases with increasing the coating surface temperature. Through modelling of heat transfer, it was shown that the coating surface temperature is smaller for substrates of higher thermal effusivity. Generally, using substrates of lower thermal effusivity and substrate preheating can result in significantly improved qualities of cold-sprayed deposits of up to a millimetre thickness.

Acknowledgments

The authors thank F. Häußler, C. Endriß, J. Carlsdotter, T. Breckwoldt, N. Németh and M. Schulze for assistance with the experiments.

References

[1] A. Papyrin, Cold Spray Technology, first ed., Elsevier, Amsterdam, 2007.

[2] H. Assadi, F. Gärtner, T. Stoltenhoff, H. Kreye, Bonding mechanism in cold gas spraying, Acta Mater 51 (2003) 4379-4394.

[3] T. Hussain, D.G. McCartney, P.H. Shipway, Impact phenomena in cold-spraying of titanium onto various ferrous alloys, Surf Coat Technol 205 (2011) 5021-5027.

[4] G. Bae, S. Kumar, S. Yoon, K. Kang, H. Na, H. Kim, C. Lee, Bonding features and associated mechanisms in kinetic sprayed titanium coatings, Acta Mater 57 (2009) 5654-5666.

[5] M. Grujicic, C.L. Zhao, W.S. DeRosset, D. Helfritch, Adiabatic shear instability based mechanism for particles/substrate bonding in the cold-gas dynamic-spray process, Mater Des 25 (2004) 681-688.

[6] T. Schmidt, F. Gärtner, H. Assadi, H. Kreye, Development of a generalized parameter window for cold spray deposition, Acta Mater 54 (2006) 729-742.

[7] H. Assadi, T. Schmidt, H. Richter, J.O. Kliemann, K. Binder, F. Gärtner, T. Klassen, H. Kreye, On Parameter selection in cold spraying, J Therm Spray Technol 20 (2011) 1161-1176.

[8] G. Bae, Y. Xiong, S. Kumar, K. Kang, C. Lee, General aspects of interface bonding in kinetic sprayed coatings, Acta Mater 56 (2008) 4858-4868.

[9] F. F. Wang, W. Y. Li, M. Yu, H. L. Liao, Prediction of critical velocity during cold spraying based on a coupled thermomechanical Eulerian model, J Therm Spray Technol 23 (2014) 60-67.

[10] H. Assadi, T. Schmidt, F. Gärtner, H. Kreye, Characteristics of particle bonding and material deposition in cold spraying, Proc. of Aerospace Materials and Manufacturing Processes: Emerging Materials, Processes, and Repair Techniques, Eds. M. Jahazi, M. Elboujdaïni and P. Patnaik, COM 2006, 1-4 October 2006, Montreal, Canada, 49-59.

[11] X. K. Suo, X.P. Guo, W.Y. Li, M.P. Planche, H.L. Liao, Investigation of deposition behavior of cold-sprayed magnesium coating, J Therm Spray Technol 21 (2012) 831-837.

[12] R. Ghelichi, S. Bagherifard, M. Guagliano, M. Verani, Numerical simulation of cold spray coating, Surf Coat Technol 205 (2011) 5294-5301.

[13] F. Raletz, M. Vardelle, G. Ezo, Critical particle velocity under cold spray conditions, Surf Coat Technol 201 (2006) 1942-1947.

[14] M. Grujicic, C.L. Zhao, C. Tong, W.S. DeRosset, D. Helfritch, Analysis of the impact velocity of powder particles in the cold-gas dynamic-spray process, Mater Sci Eng A 368 (2004) 222-230.

[15] D. Goldbaum, J. M. Shockley, R. R. Chromik, A. Rezaeian, S. Yue, J.-G. Legoux, E. Irissou, The effect of deposition conditions on adhesion strength of Ti and Ti6Al4V cold spray splats, J Therm Spray Technol 21 (2012) 288-303.

[16] R. C. Dykhuizen, M. F. Smith, Gas dynamic principles of cold spray, J Therm Spray Technol 7 (1998) 205-212.

[17] D. L. Gilmore, R. C. Dykhuizen, R. A. Neiser, T. J. Roemer, M. F. Smith, Particle velocity and deposition efficiency in the cold spray process, J Therm Spray Technol 8 (1999) 576-582.

[18] R. C. Dykhuizen, M. F. Smith, D. L. Gilmore, R. A. Neiser, X. Jiang, S. Sampath, Impact of high velocity cold spray particles, J Therm Spray Technol 8 (1999) 559-564.

[19] P. C. King, G. Bae, S. H. Zahiri, M. Jahedi, C. Lee, An experimental and finite element study of cold spray copper impact onto two aluminum substrates, J Therm Spray Technol 19 (2010) 620-634.

[20] D. K. Christoulis, S. Guetta, V. Guipont, M. Jeandin, The influence of the substrate on the deposition of cold-sprayed titanium: An experimental and numerical study, J Therm Spray Technol 20 (2011) 523-533.

[21] M. Villa Vidaller, A. List, F. Gärtner, T. Klassen, S. Dosta, J. M. Guilemany, Single impact bonding of cold sprayed Ti-6Al-4V powders on different substrates, J Therm Spray Technol 24 (2015) 644-658.

[22] A. Manap, O. Nooririnah, H. Misran1, T. Okabe, K. Ogawa, Experimental and SPH study of cold spray impact between similar and dissimilar metals, Surf Eng 30 (2014) 335-341.

[23] S. Yin, X. Suo, J. Su, Z. Guo, H. Liao, X. Wang, Effects of substrate hardness and spray angle on the deposition behavior of cold-sprayed Ti particle, J Therm Spray Technol 23 (2014) 76-83.

[24] R. Drehmann, T. Grund, T. Lampke, B. Wielage, K. Manygoats, T. Schucknecht, D. Rafaja, Splat formation and adhesion mechanisms of cold gas-sprayed Al coatings on Al2O3 substrates, J Therm Spray Technol 23 (2014) 68-75.

[25] M. Fukumoto, H. Wada, K. Tanabe, M. Yamada, E. Yamaguchi, A. Niwa, M. Sugimoto, M. Izawa, Effect of substrate temperature on deposition behavior of copper particles on substrate surfaces in the cold spray process, J Therm Spray Technol 16 (2007) 643-650.

[26] Y. Watanabe, C. Yoshida, K. Atsumi, M. Yamada, M. Fukumoto, Influence of substrate temperature on adhesion strength of cold-sprayed coatings, J Therm Spray Technol 24 (2015) 86-91.

[27] X. K. Suo, M. Yu, W. Y. Li, M. P. Planche, H. L. Liao, Effect of substrate preheating on bonding strength of cold-sprayed Mg coatings, J Therm Spray Technol 21 (2012) 1091-1098.

[28] M. M. Sharma, T. J. Eden, B. T. Golesich, Effect of surface preparation on the microstructure, adhesion, and tensile properties of cold-sprayed aluminum coatings on AA2024 substrates, J Therm Spray Technol 24 (2015) 410-422.

[29] K. R. Ernst, J. Braeutigam, F. Gärtner, T. Klassen, Effect of substrate temperature on cold-gas-sprayed coatings on ceramic substrates, J Therm Spray Technol 22 (2013) 422-432.

[30] X. Zhou, X. Wu, J. Wang, and J. Zhang, Numerical investigation of the rebounding and the deposition behavior of particles during cold spraying, Acta Metall Sinica (Engl. Lett.) 24 (2011) 43-53.

[31] A. List, F. Gärtner, T. Schmidt, T. Klassen, Impact conditions for cold spraying of hard metallic glasses, J Therm Spray Technol 21 (2012) 531-540.

[32] M. Villa Vidaller, F. Häußler, H. Assadi, F. Gärtner, T. Klassen, Influence of substrate on cold sprayed titanium coatings, Proceedings of the International Thermal Spray Conference (May 11-14, 2015, Long Beach, California, USA) 1047-1054.

[33] J. Voyer, T. Stoltenhoff, T. Schmidt, H. Kreye, Method and potential of the cold spray process, Proc. 6. Kolloqium Hochgeschwindigkeits - Flammspritzen, Erding, Germany, November 27 – 28, 2003, (Ed.: P. Heinrich), Gemeinschaft Thermisches Spritzen e.V., Unterschleißheim, Germany (2003) 39-47.

[34] H. Assadi, F. Gärtner, T. Stoltenhoff, H. Kreye, Application of Analytical Methods for Understanding and Optimization of the Cold Spray Process, H. Assadi, F. Gärtner, T. Stoltenhoff, H. Kreye, Proc. 6. Kolloqium Hochgeschwindigkeits - Flammspritzen, Erding, Germany, November 27 – 28, 2003, (Ed.: P. Heinrich), Gemeinschaft Thermisches Spritzen e.V., Unterschleißheim, Germany (2003) 49-59.

[35] J. Wu, H. Fang, S. Yoon, H. Kim, C. Lee, Measurement of particle velocity and characterization of deposition in aluminum alloy kinetic spraying process, Appl Surf Sci 252 (2005) 1368-1377.

[36] T. Stoltenhoff, H. Kreye, H. J. Richter, An analysis of the cold spray process and its coatings, J Therm Spray Technol 11 (2002) 542-550.

[37] F. Gärtner, T. Stoltenhoff, T. Schmidt, H. Kreye, The cold spray process and its potential for industrial applications, J Therm Spray Technol 15 (2006) 223-232.

[38] K. Binder, J. Gottschalk, M. Kollenda, F. Gärtner, T. Klassen, Influence of impact angle and gas temperature on mechanical properties of titanium cold spray deposits, J Therm Spray Technol 20 (2011) 234-242.

[39] J.-G. Legoux, E. Irissou, C. Moreau, Effect of substrate temperature on the formation mechanism of cold-sprayed aluminum, zinc and tin coatings, J Therm Spray Technol 16 (2007) 619-626.

[40] Y. Xiong, G. Bae, X. Xiong, C. Lee, The effects of successive impacts and cold welds on the deposition onset of cold spray coatings, J Therm Spray Technol 19 (2010) 575-585.

[41] S. Yin, X. F. Wang, W. Y. Li, H. Jie, Effect of substrate hardness on the deformation behavior of subsequently incident particles in cold spraying, Appl Surf Sci 257 (2011) 7560-7565.

[42] T. Stoltenhoff, C. Borchers, F. Gärtner, H. Kreye, Microstructures and key properties of cold-sprayed and thermally sprayed copper coatings, Surf Coat Technol 200 (2006) 4947-4960.

[43] S. Krebs, F. Gärtner, T. Klassen, Cold spraying of Cu-Al-Bronze for cavitation protection in marine environments, J Therm Spray Technol 45 (2014) 708-716.

[44] S. Rech, A. Trentin, S. Vezzu, J.-G. Legoux, E. Irissou, M. Guagliano, Influence of pre-heated Al 6061 substrate temperature on the residual stresses of multipass Al coatings deposited by cold spray, J Therm Spray Technol 20 (2011) 243-251.

[45] F. Gärtner, T. Stoltenhoff, J. Voyer, H. Kreye, S. Riekehr, M. Koçak, Mechanical properties of cold-sprayed and thermally sprayed copper coatings, Surface and Coatings Technology 200 (2006) 6770-6782.

[46] Y. Y. Wang, Y. Liu, G.J. Yang, J. J. Feng, K. Kusumoto, Effect of microstructure on the electrical properties of nano-structured TiN coatings deposited by vacuum cold spray, J Therm Spray Technol 19 (2010) 1231-1237.

[47] K. Binder, Kaltgasspritzen von ermüdungsfesten Titanschichten: Thesis, Helmut-Schmidt-Universität, Hamburg, Shaker Verlag, Aachen, 2012.

[48] G. Sundararajan, N. M. Chavan, G. Sivakumar, P. S. Phani, Evaluation of parameters for assessment of inter-splat bond strength in cold-sprayed coatings, J Therm Spray Technol 19 (2010) 1255-1266.

[49] K. Binder, F. Gärtner, T. Klassen, Cold spraying of titanium using enhanced conditions and optimized nozzles, Proc. ITSC 2011, Hamburg, September 27 – 29, 2011, DVS-Berichte Volume 276, DVS Media GmbH, Düsseldorf 2011, p. 879-884.

[50] T. Schmidt, F. Gaertner, H. Kreye, New Developments in Cold Spray Based on Higher Gas- and Particle Temperatures, J. Therm. Spray. Technol. 15 (2006) 488–494.

[51] G. R. Johnson, W. H. Cook, A constitutive model and data for metals subjected to large strains, high strain rates and high temperatures, 7th Int Symp on Ballistics, The Netherlands (1983) 541-547.

[52] www.matweb.com

[53] H. Assadi, H. Kreye, F. Gärtner, T. Klassen, Cold spraying – A materials perspective, Acta Mater 116 (2016) 382-407.

[54] S. Yin, X. F. Wang, W. Y. Li, X. P. Guo, Examination on substrate preheating process in cold gas dynamic spraying, J Therm Spray Technol 20 (2011) 852-859.

[55] W. Y. Li, S. Yin, X. Guo, H. Liao, X. F. Wang, C. Coddet, An investigation on temperature distribution within the substrate and nozzle wall in cold spraying by numerical and experimental methods, J Therm Spray Technol 21 (2012) 41-48.

[56] A. N. Ryabinin, E. Irissou, A. McDonald, J. G. Legoux, Simulation of gas-substrate heat exchange during cold-gas dynamic spraying, Int J Therm Sciences 56 (2012) 12-18.

[57] A. G. McDonald, A. N. Ryabinin, E. Irissou, J. G. Legoux, Gas-Substrate Heat Exchange During Cold-Gas Dynamic Spraying, J Therm Spray Technol 22 (2013) 391-397.

[58] S. Yin, X. F. Wang, W. Y. Li, Y. Li, Numerical Study on the Effect of Substrate Size on the Supersonic Jet Flow and Temperature Distribution Within the Substrate in Cold Spraying, J Therm Spray Technol 21 (2012) 628-635.

[59] S. Yin, M. Meyer, W. Y. Li, H. Liao, R. Lupoi, Gas Flow, Particle Acceleration, and Heat Transfer in Cold Spray: A review, J Therm Spray Technol 25 (2016) 1-23.

[60] S. Yin, X. F Wang, W. Li, X. Guo, Examination on substrate preheating process in cold gas dynamic spraying, J Therm Spray Technol 20 (2011) 852-859.

[61] Z. Arabgol, H. Assadi, T. Schmidt, F. Gärtner, T. Klassen, Analysis of thermal history and residual stress in cold-sprayed coatings, J Therm Spray Technol 23 (2014) 84-90.

[62] C. Borchers, F. Gärtner, T. Stoltenhoff, H. Kreye, Formation of persistent dislocation loops by ultra-high strain-rate deformation during cold spraying, Acta Mater 53 (2005) 2991-3000.

[63] Yongzhou Wang, Fundamentals of Recrystallization in Titanium alloys, Master Thesis 2014, University of Manchester.

[64] R.J. Contieria, M. Zanotellob, R. Carama, Recrystallization and grain growth in highly cold worked CP-Titanium, Materials Science and Engineering A 527 (2010) 3994–4000.

[65] K. H. Zum Gahr, G. T. Eldis, Abrasive wear of white cast iron, Wear 64 (1980) 175-194.

[66] D. Goldbaum, R. Chromik, S. Yue, E. Irissou, J.-G. Legoux, Mechanical property mapping of cold sprayed Ti splats and coatings, J Therm Spray Technol 20 (2011) 486-496.

[67] P. C. King, S. Zahiri, M. Jahedi, J. Friend, Aluminium coating of lead zirconate titanate-A study of cold spray variables, Surf Coat Technol 205 (2010) 2016-2022.

[68] P. C. King, A. J. Poole, S. Horne, R. Nys , S. Gulizia, M. Jahedi, Embedment of copper particles into polymers by cold spray, Surf Coat Technol 216 (2013) 60-67.

Table 1. Properties of materials considered in this study.

Property		**Unit**	**Cu**	**Steel**	**Ti**	**Al**	**AlMg3**	**Al7075**
Conductivity (k)		W/m/K	385	16.2	16.4	210	140	130
Density (ρ)		kg/m^3	890	8000	4500	2699	2650	2810
Young's modulus (E)		GPa	110	193	116	68	70	71.7
Poison's ratio (μ)		-	0.35	0.24	0.34	0.36	0.33	0.33
Tensile strength (UTS)		MPa	200	500	350	-	-	-
Thermal expansion (α)		10^{-5}/K	1.64	1.69	8.90	2.40	2.4	2.36
Specific heat (c_p)		J/kg/K	385	500	523	900	960	960
Melting Temp. (T_m)		K	135	1673	1941	933	-	-
Thermal effusivity (e)		kJ/m^2/K/s$^{1/2}$	36.3	8.1	6.2	22. 6	18.9	18.7
Johnson - Cook parameters	A	MPa	90	1079	806.57	148	-	496
	B	MPa	292	1120	481.61	345	-	310
	n	-	0.31	0.58	0.319	0.183	-	0.3
	c	-	0.02	0.016	0.0194	0.001	-	0.0001
	m	-	1.09	1.13	0.655	0.895	-	1.2

Figure Captions

Figure 1. The correlation between electrical conductivity and in-plane ultimate tensile strength of cold-sprayed titanium coatings, as obtained for different spray angles and nozzle geometries. Data from [47a].

Figure 2. SEM micrographs of the titanium powder, showing (left) morphology and (right) cross-section of the particles.

Figure 3. SEM and optical micrographs of the copper powder, showing (left) morphology and (right) cross-section of the particles.

Figure 4. Setup for modelling of particle impact (micro model) and heat transfer (macro model) during cold spraying.

Figure 5. Cross section of (a) copper and (b) titanium coatings cold sprayed with nitrogen on different substrates at room temperature, under spraying conditions corresponding to $\eta = 1.17$ (T_{gas} = 320 °C, p_{gas} = 30 bar) and $\eta = 1.16$ (T_{gas} = 800 °C, p_{gas} = 40 bar), respectively.

Figure 6. Measured hardness of the copper and titanium coatings cold sprayed, using nitrogen as process gas, on different substrates of different initial substrate temperatures. The spraying conditions correspond to $\eta = 1.17$ for copper (T_{gas} = 320 °C, p_{gas} = 30 bar), and 1.16 for titanium (T_{gas} = 800 °C, p_{gas} = 40 bar).

Figure 7. Electrical conductivities measured from the polished top surface of (~1 mm) thick cold-sprayed copper (a) and titanium coatings (b) on different substrate materials for various initial temperatures. Values are expressed as relative increase in conductivity with reference to that of copper and/or titanium coatings on copper substrate at room temperature.

Figure 8. Results of particle impact simulations, showing the final deformation morphologies and distribution of the equivalent plastic strain in the particle, coating and substrate, for

different coating thicknesses. The impact velocity and the overall temperature are fixed for all cases to 450 m/s and 25 °C, respectively, corresponding to $\eta = 1.15$.

Figure 9. Profiles of the plastic strain on the meridian path along the particle surface (distance from the first point of contact), showing the effect of the already deposited coating thickness – (a) 5 µm, (b) 10 µm, (c) 25 µm – and the substrate material on the extent and of highly deformed regions (e.g. with strains > 2) for the cases shown in Fig. 8. The solid lines correspond to steel substrates, the dashed lines to aluminium substrates.

Figure 10. Calculated fraction of particle surface area with large (>2) equivalent plastic strains (PEEQ) as a function of the thickness of the previously deposited layer, for different substrate materials. The impact velocity and the overall temperature are set to 450 m/s and 25 °C, respectively. Beyond 50 µm coating thickness, which is equivalent to just a few layers of particle splats, the effect of the substrate material at fixed temperature vanishes.

Figure 11. Calculated fraction of surface area with large (>2) equivalent plastic strains (PEEQ) on particle, substrate, and the mean value, as a function of coating surface temperature, for cold spraying of titanium. The pre-deposited coating thickness is assumed to be 300 µm in all cases.

Figure 12. Results of heat transfer simulations, showing the temperature of the coating surface under the spray jet, as a function of the initial substrate temperature, for different substrate materials. The thickness of the titanium coating is assumed to be 1 mm. The spraying conditions and the respective heat transfer parameters are identical for all cases. The lines correspond to the analytical formula, Eq. (5).

Figure 13. Measured conductivity of titanium coatings as a function of (a) the temperature dependent tensile strength of the substrate, and (b) the coating surface temperature, for cold spraying onto different substrate materials (copper, titanium, steel) of various initial

temperatures. The coefficient of determination is significantly higher for the latter case (b), underlining the role of coating surface temperature as the determining factor in coating properties.

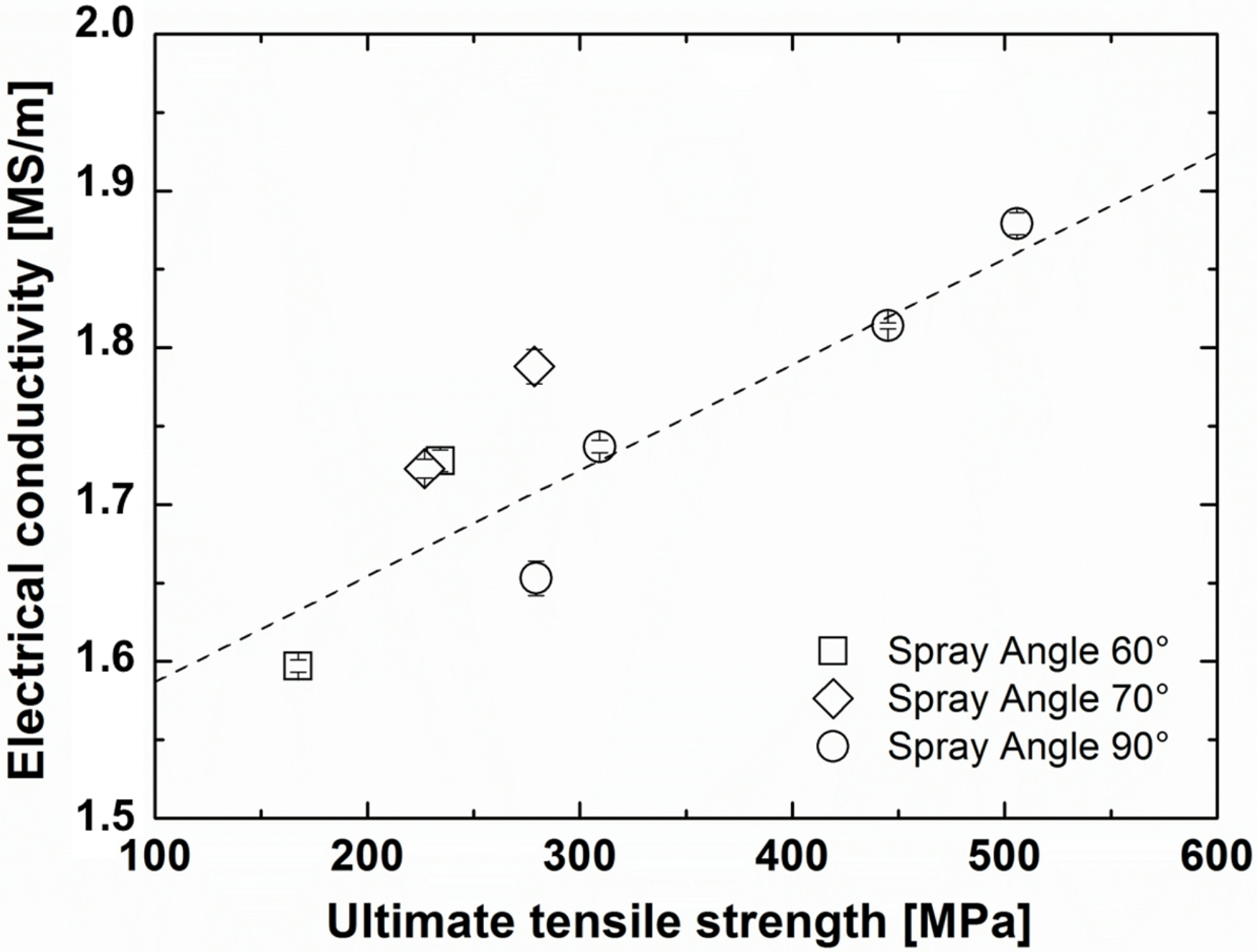
Electrical conductivity [MS/m]
2.0
1.9
1.8
1.7
1.6
1.5
100
200
300
400
500
600
Ultimate tensile strength [MPa]
Spray Angle 60°
Spray Angle 70°
Spray Angle 90°

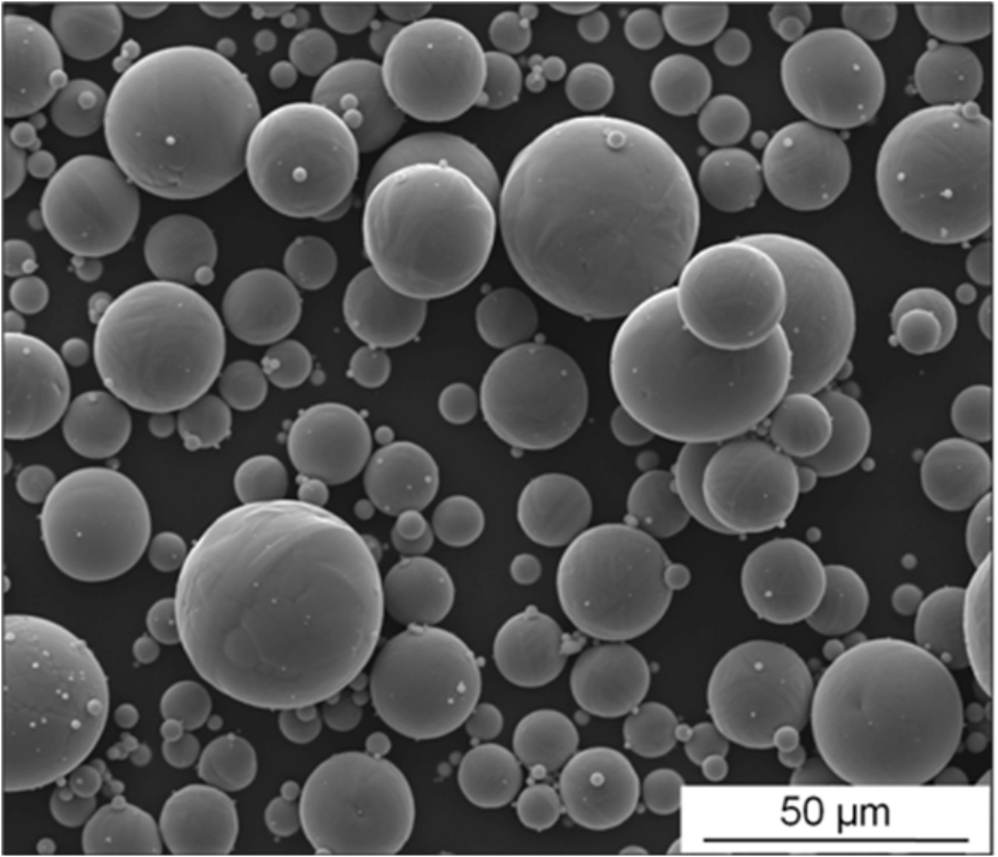
50 µm

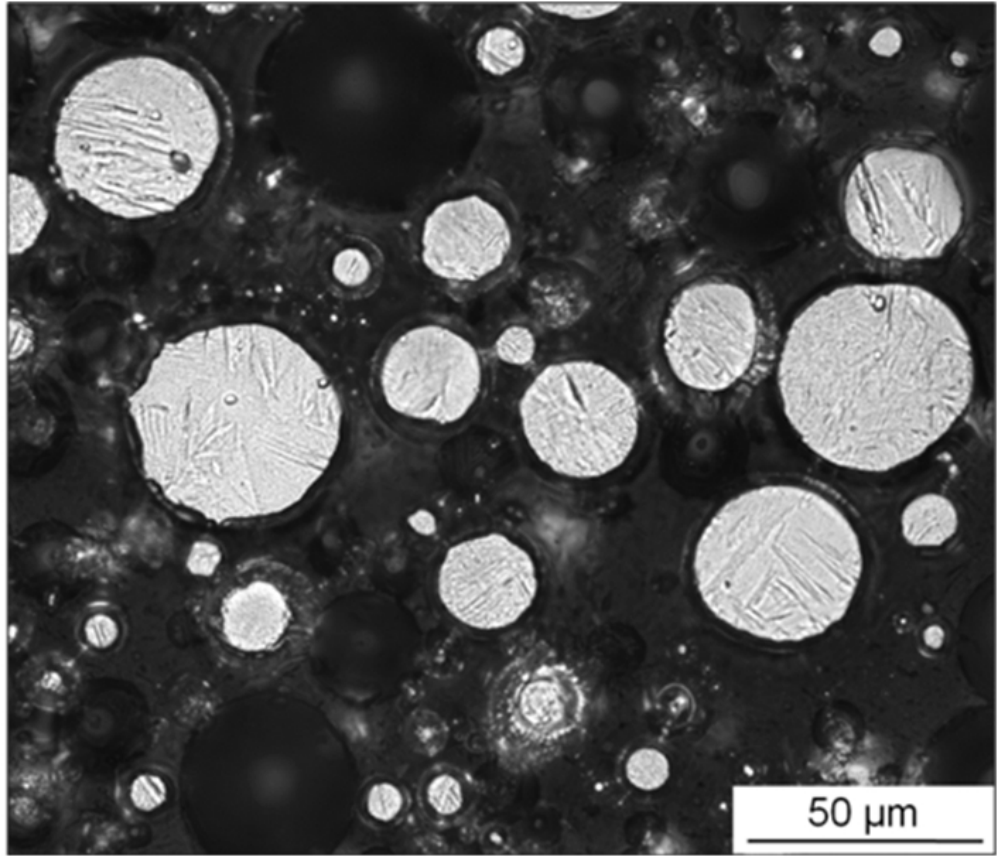
50 µm

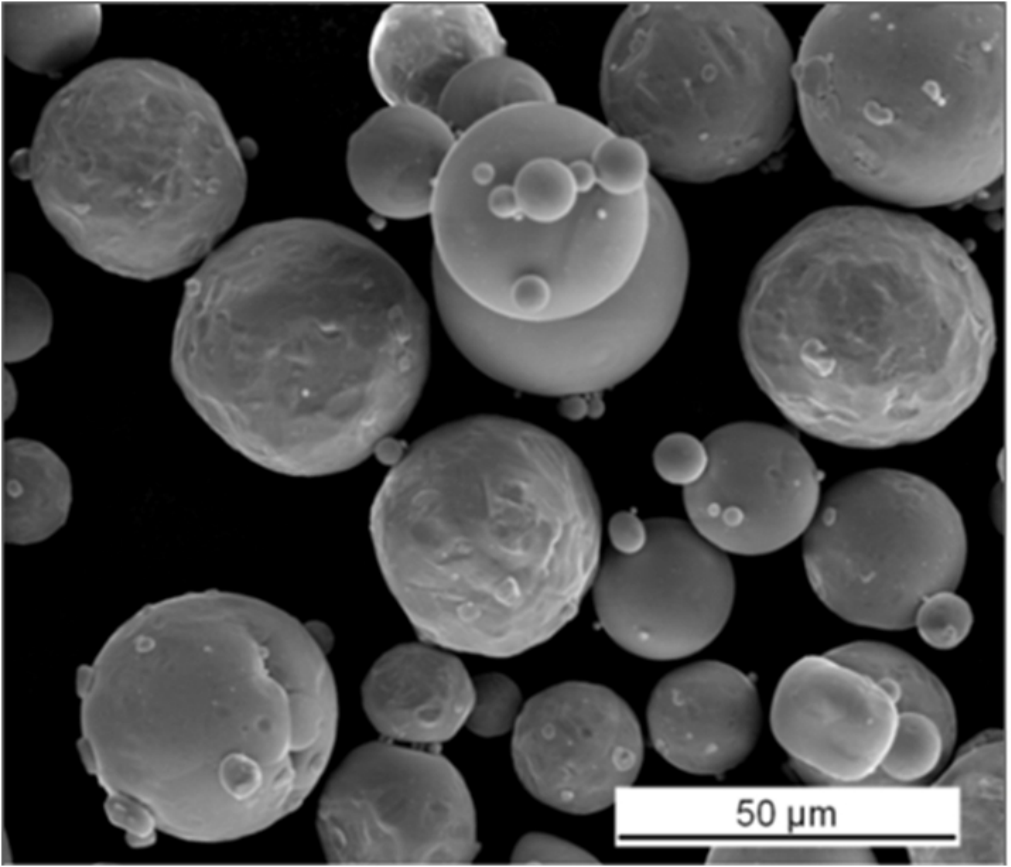
50 µm

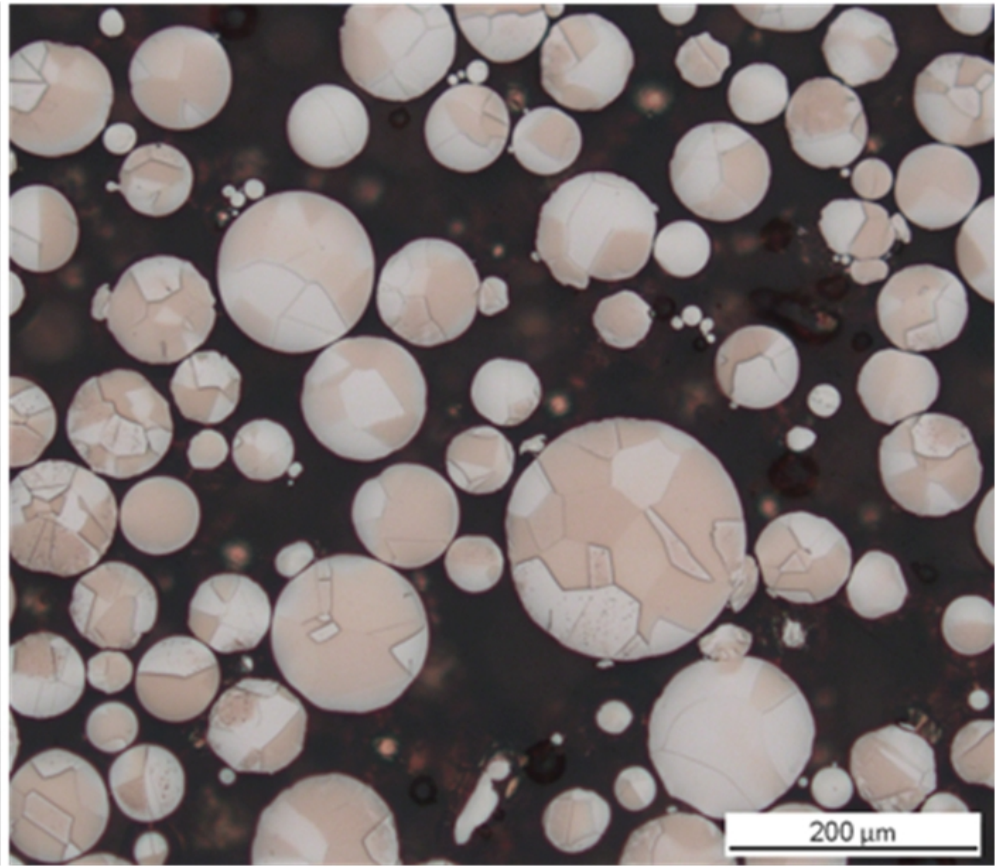
200 µm

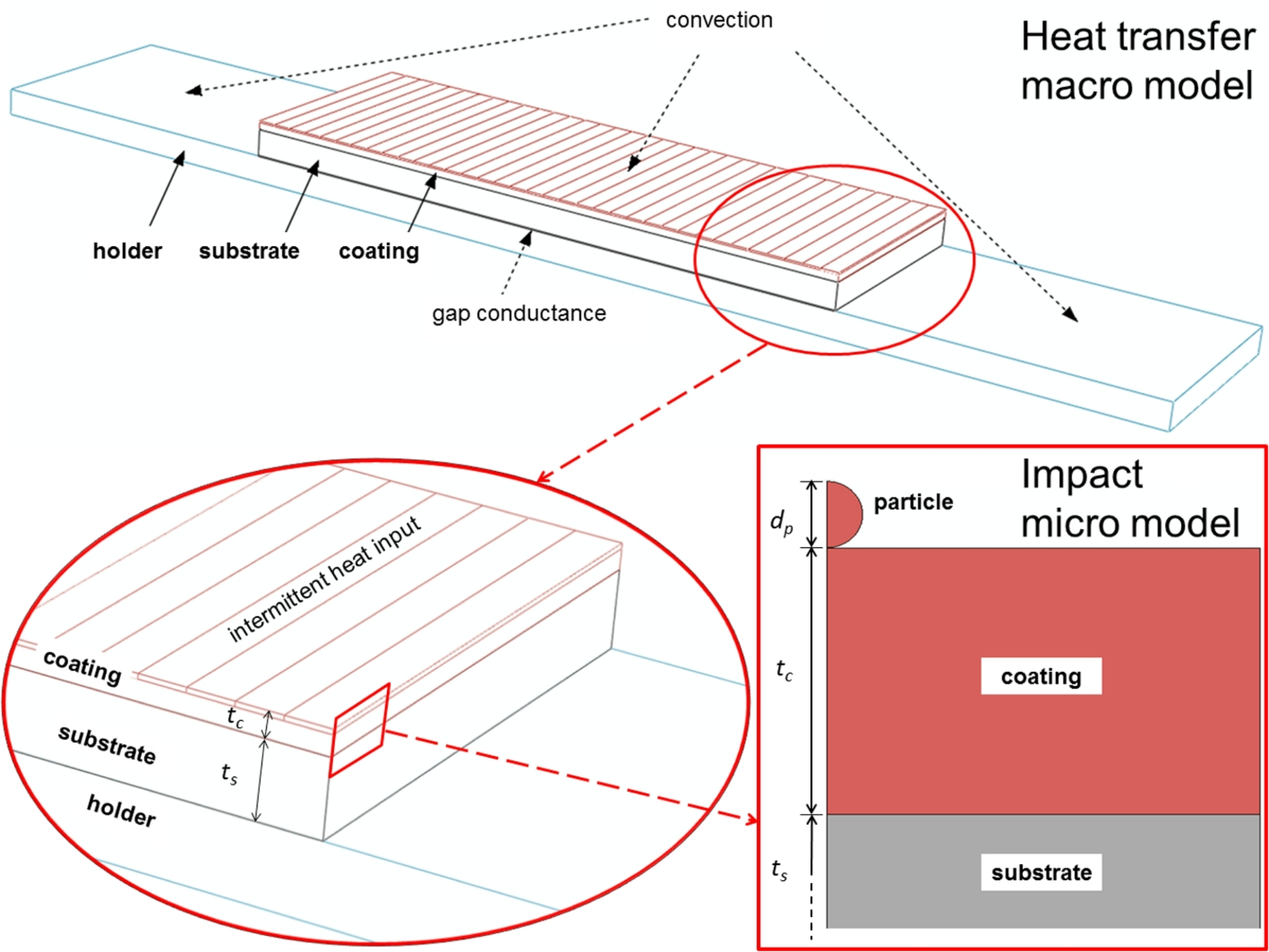
Heat transfer
macro model
convection
holder
substrate
coating
gap conductance
intermittent heat input
coating
substrate
holder
t_c
t_s
Impact
micro model
particle
d_p
t_c
coating
t_s
substrate

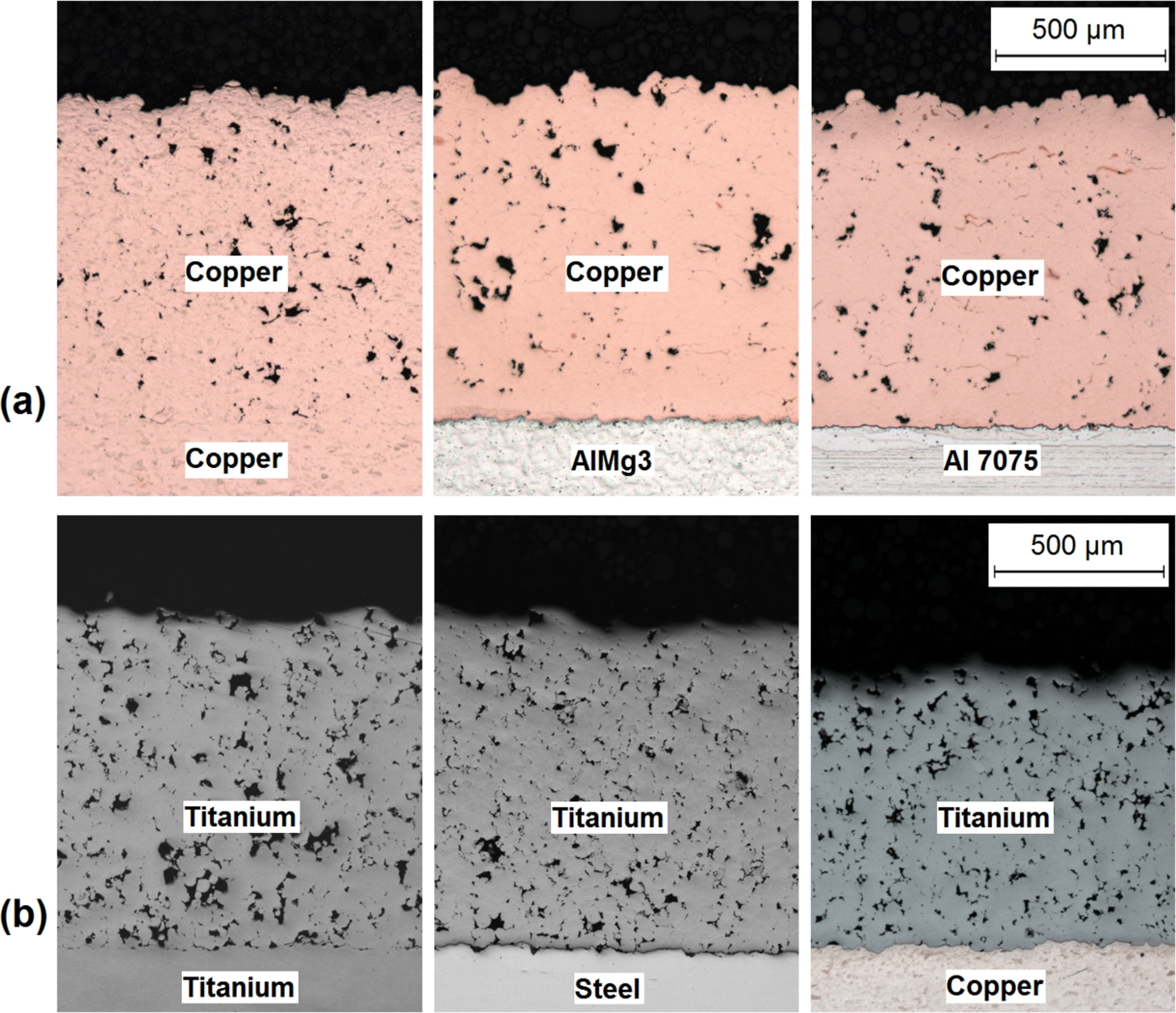
(a)
Copper
Copper
Copper
AlMg3
Copper
Al 7075
500 µm
(b)
Titanium
Titanium
Titanium
Steel
Titanium
Copper
500 µm

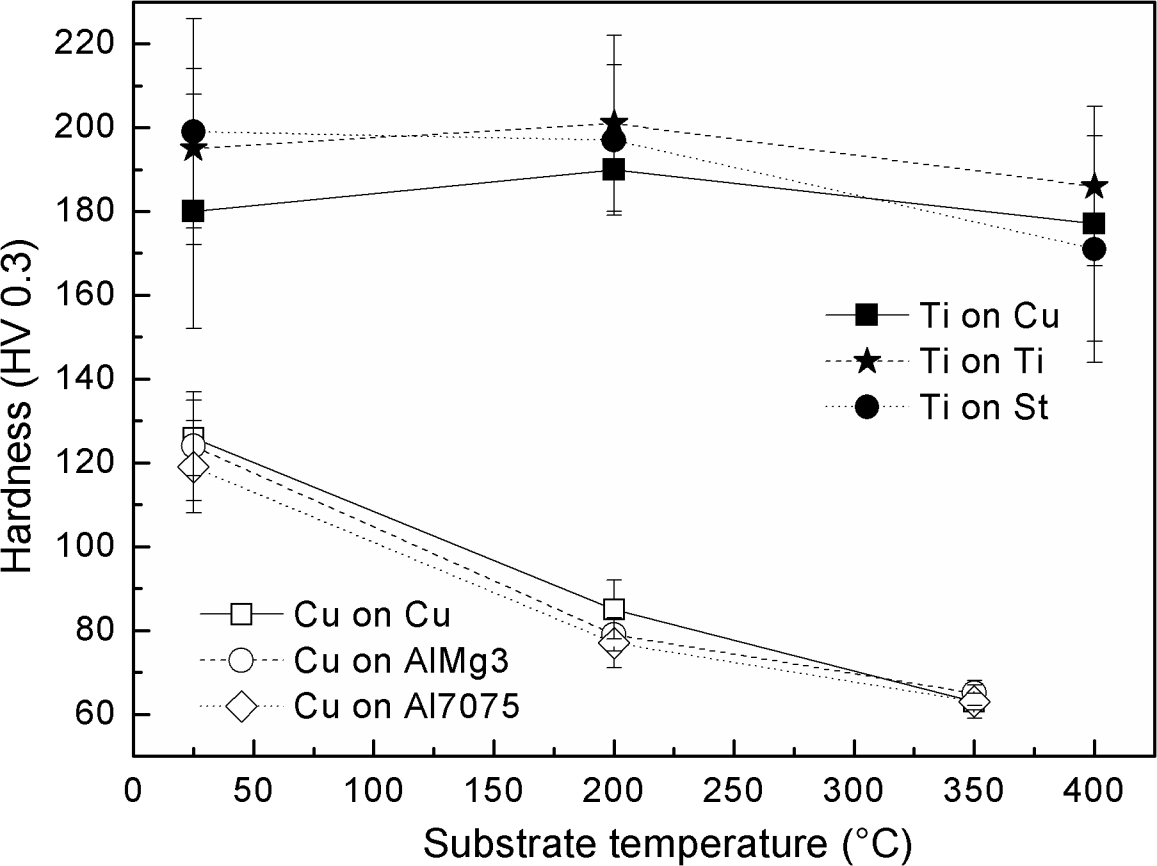
Hardness (HV 0.3)
220
200
180
160
140
120
100
80
60
0
50
100
150
200
250
300
350
400
Substrate temperature (°C)
Ti on Cu
Ti on Ti
Ti on St
Cu on Cu
Cu on AlMg3
Cu on Al7075

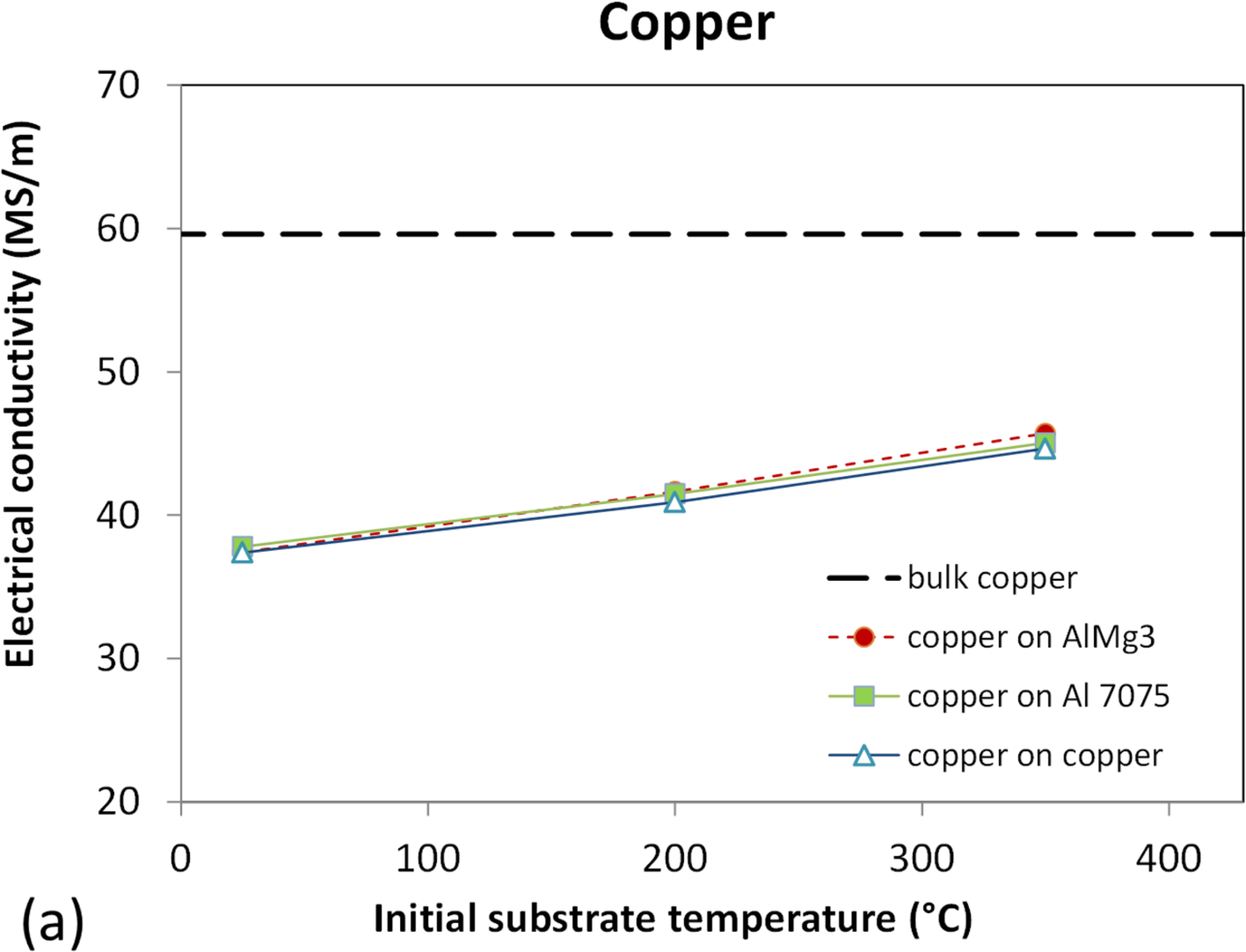
Copper
70
60
50
40
30
20
Electrical conductivity (MS/m)
0
100
200
300
400
Initial substrate temperature (°C)
bulk copper
copper on AlMg3
copper on Al 7075
copper on copper
(a)

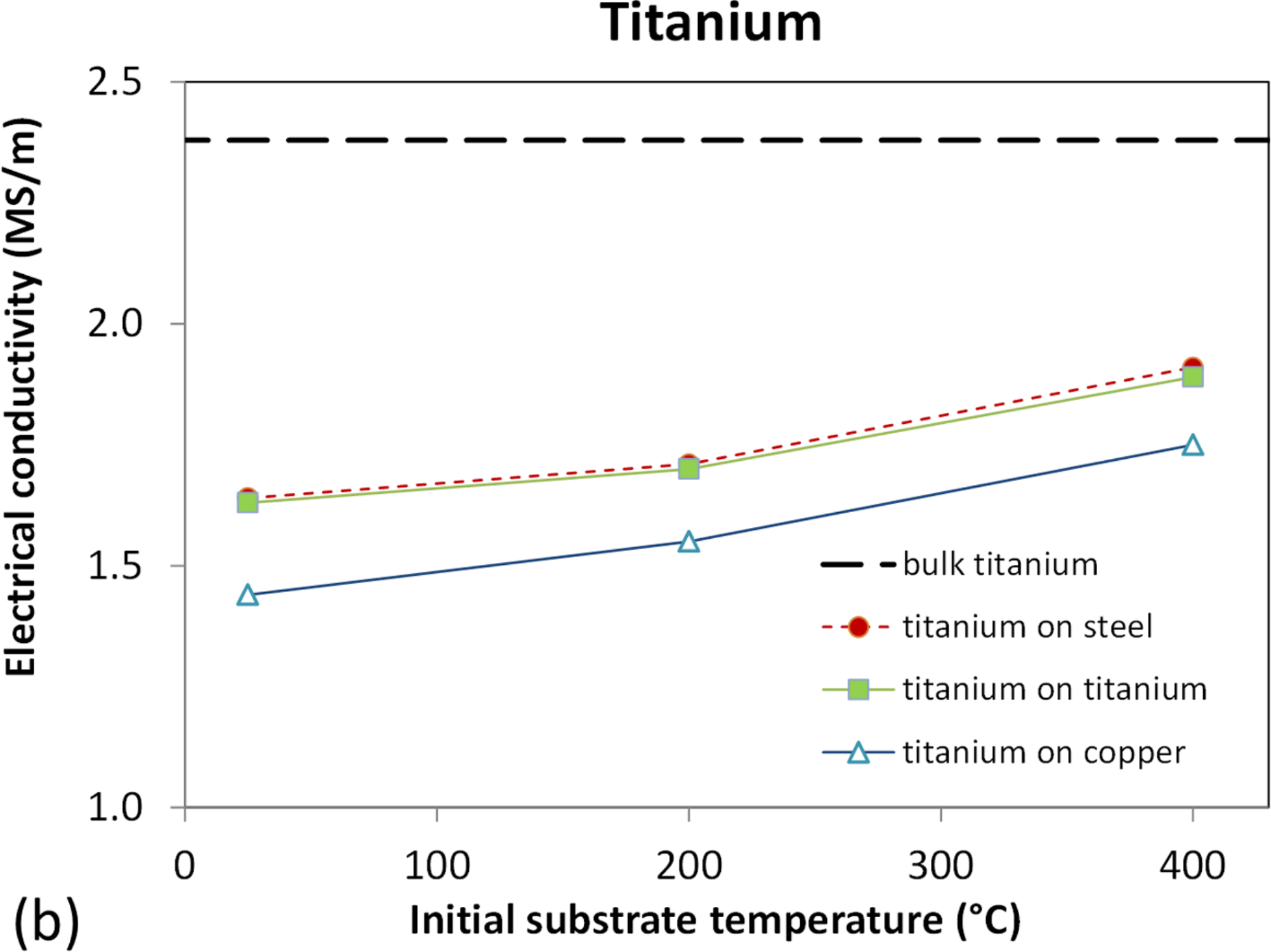
Titanium
Electrical conductivity (MS/m)
2.5
2.0
1.5
1.0
0
100
200
300
400
Initial substrate temperature (°C)
bulk titanium
titanium on steel
titanium on titanium
titanium on copper

(b)

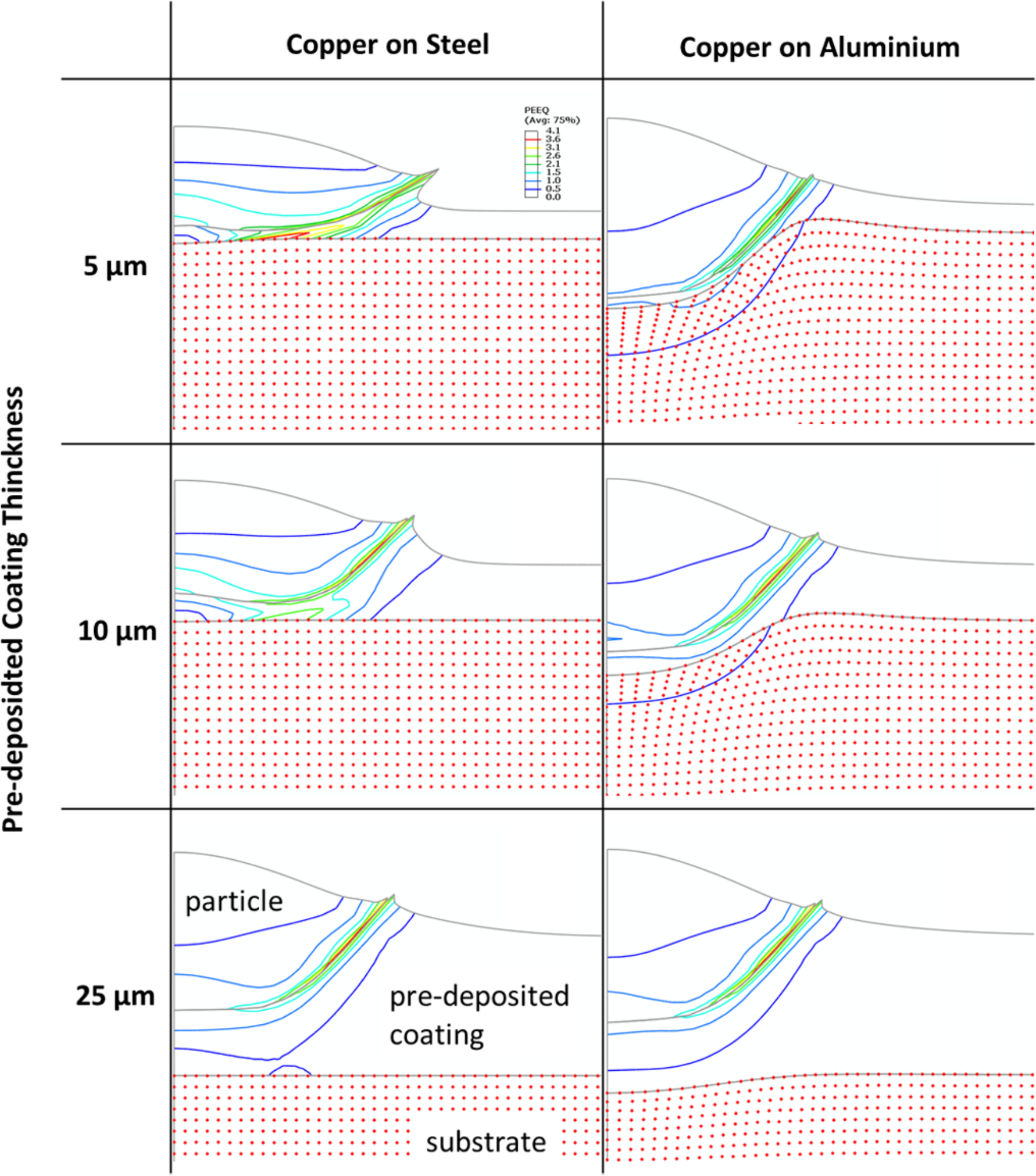
Copper on Steel
Copper on Aluminium
Pre-deposidted Coating Thinckness
5 µm
10 µm
25 µm
PEEQ
(Avg: 75%)
4.1
3.6
3.1
2.6
2.1
1.5
1.0
0.5
0.0
particle
pre-deposited
coating
substrate

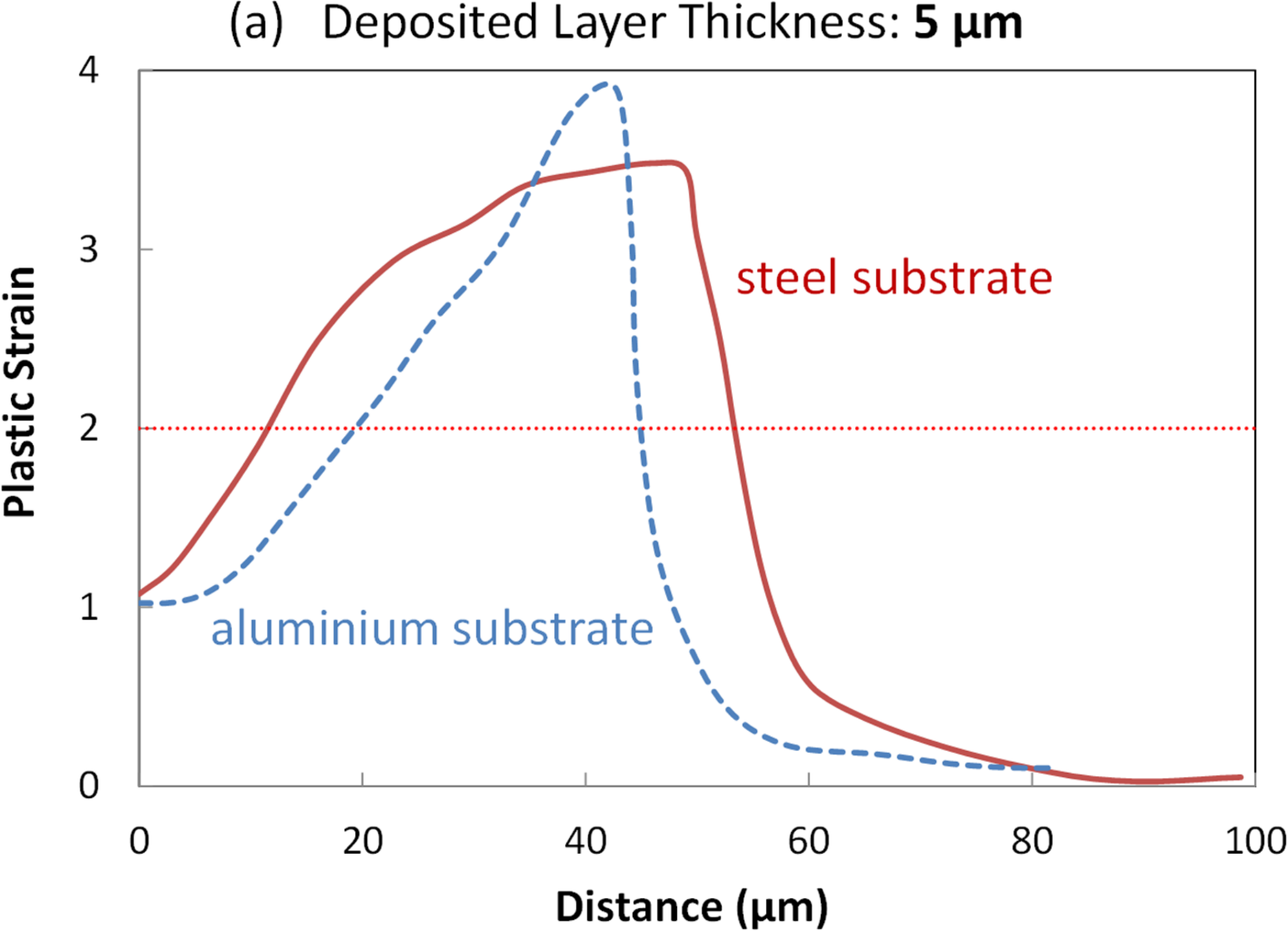
(a) Deposited Layer Thickness: 5 µm
Plastic Strain
4
3
2
1
0
0
20
40
60
80
100
Distance (µm)
steel substrate
aluminium substrate

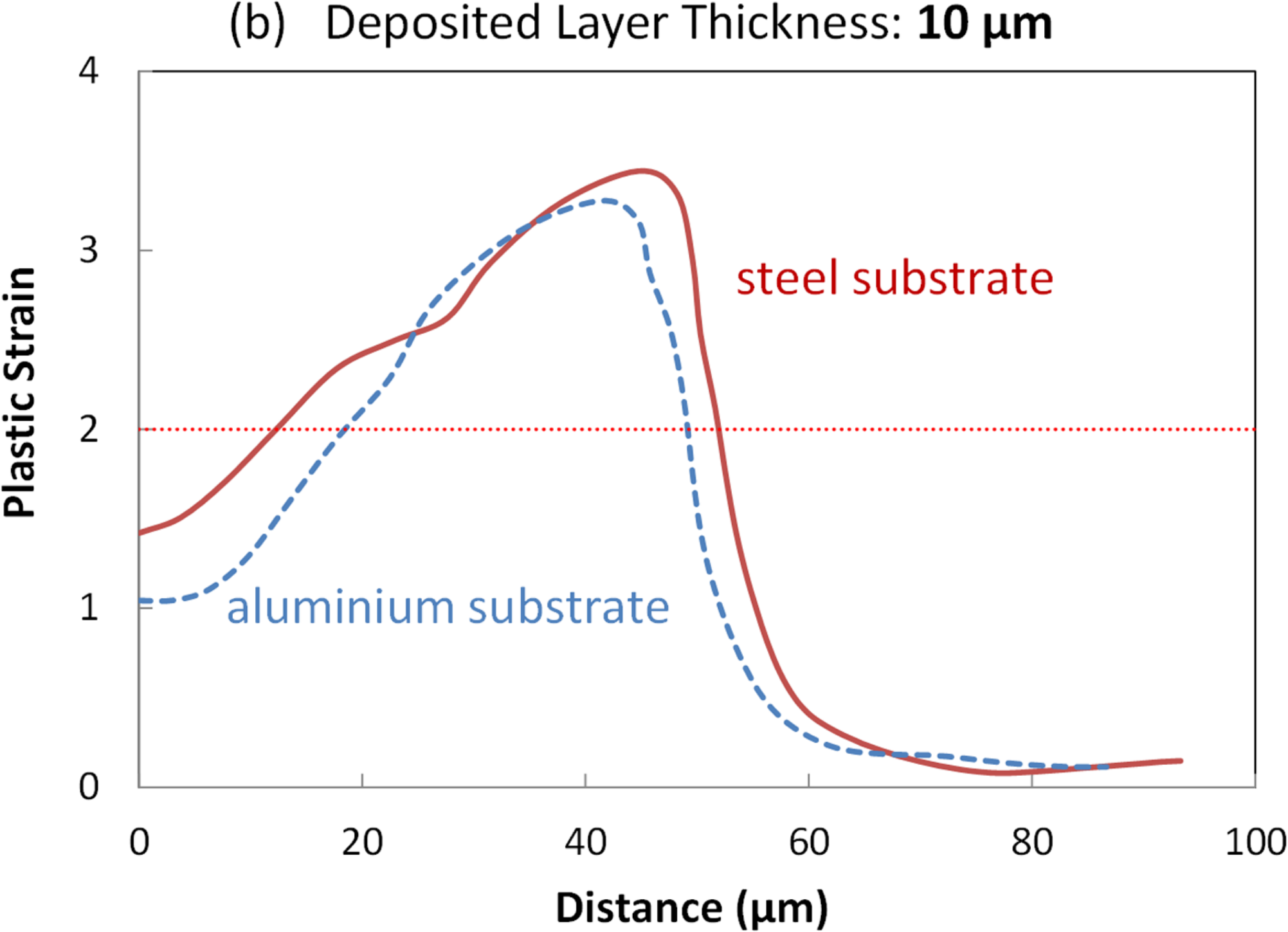
(b) Deposited Layer Thickness: 10 µm
Plastic Strain
4
3
2
1
0
steel substrate
aluminium substrate
0
20
40
60
80
100
Distance (µm)

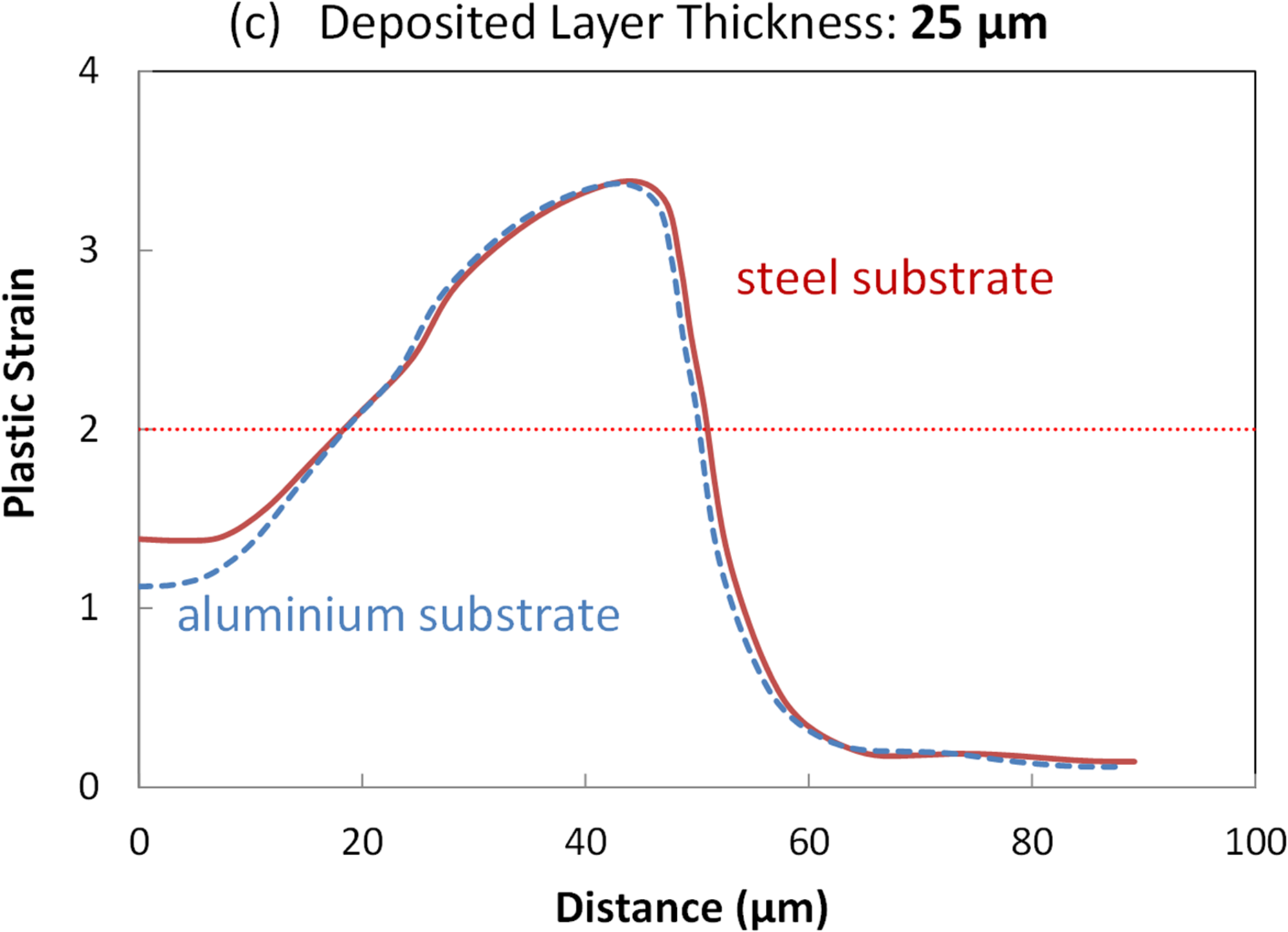
(c) Deposited Layer Thickness: 25 µm
Plastic Strain
4
3
2
1
0
steel substrate
aluminium substrate
0
20
40
60
80
100
Distance (µm)

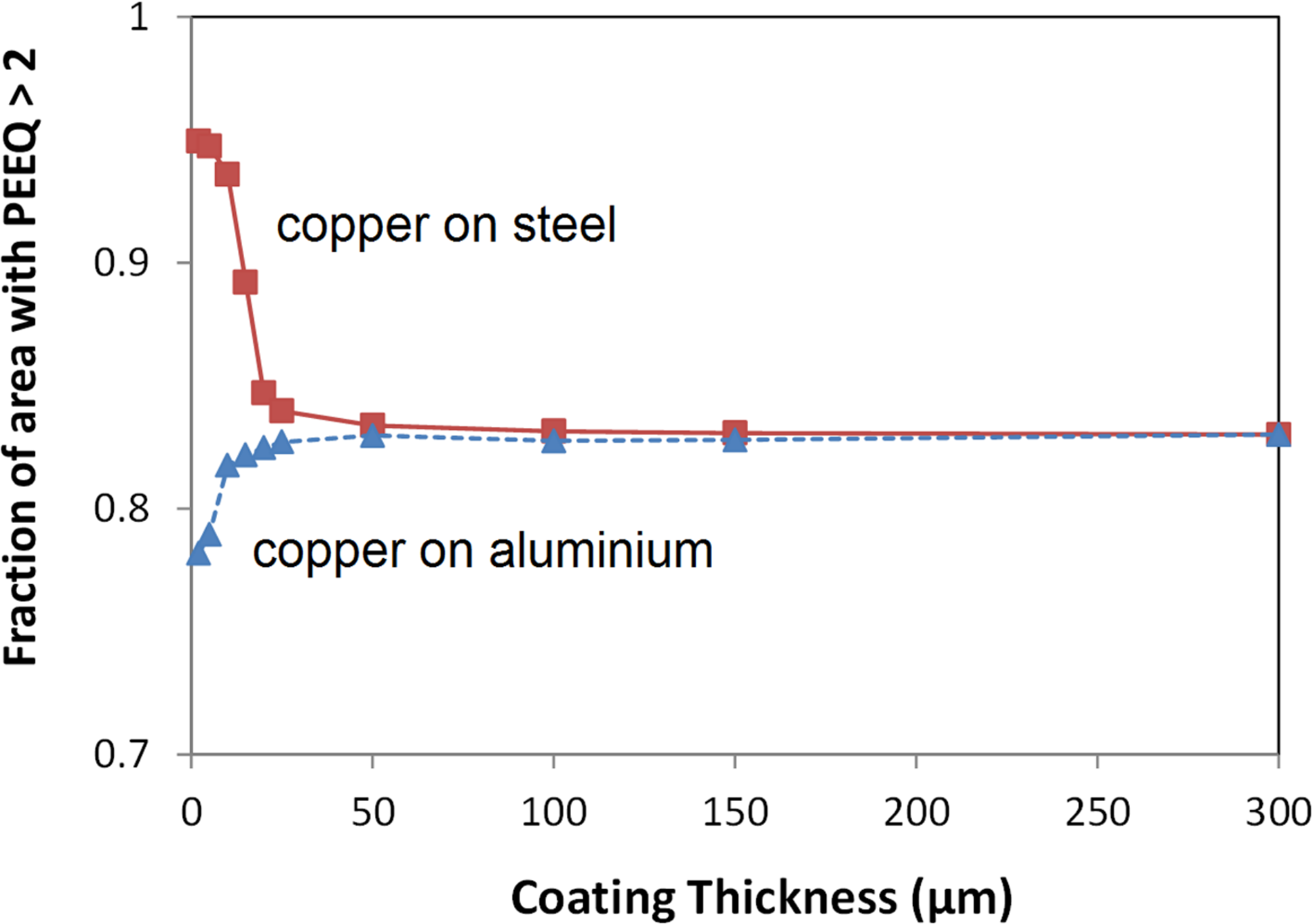
Fraction of area with PEEQ > 2
1
0.9
0.8
0.7
copper on steel
copper on aluminium
0
50
100
150
200
250
300
Coating Thickness (µm)

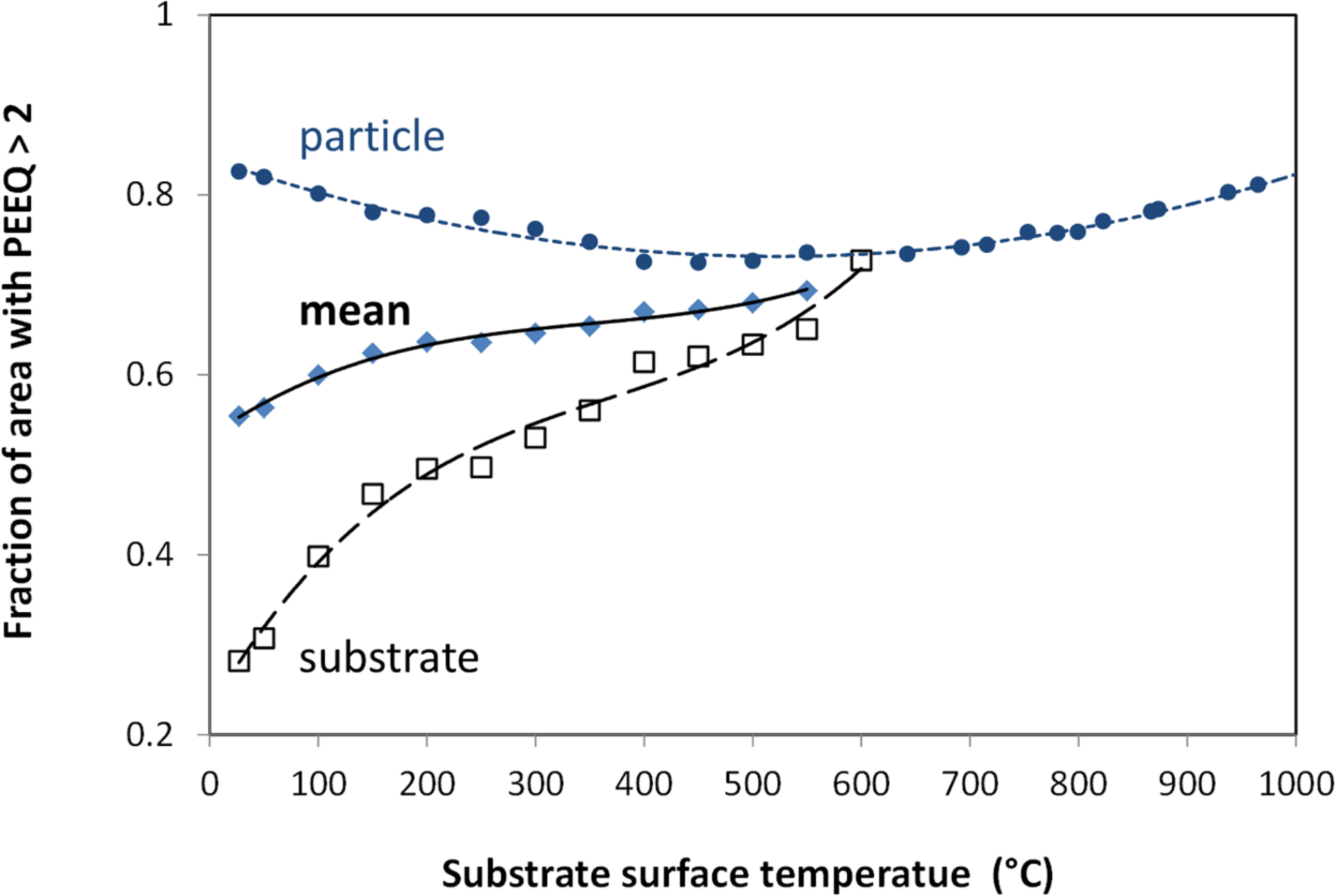
Fraction of area with PEEQ > 2
1
0.8
0.6
0.4
0.2
particle
mean
substrate
0
100
200
300
400
500
600
700
800
900
1000
Substrate surface temperatue (°C)

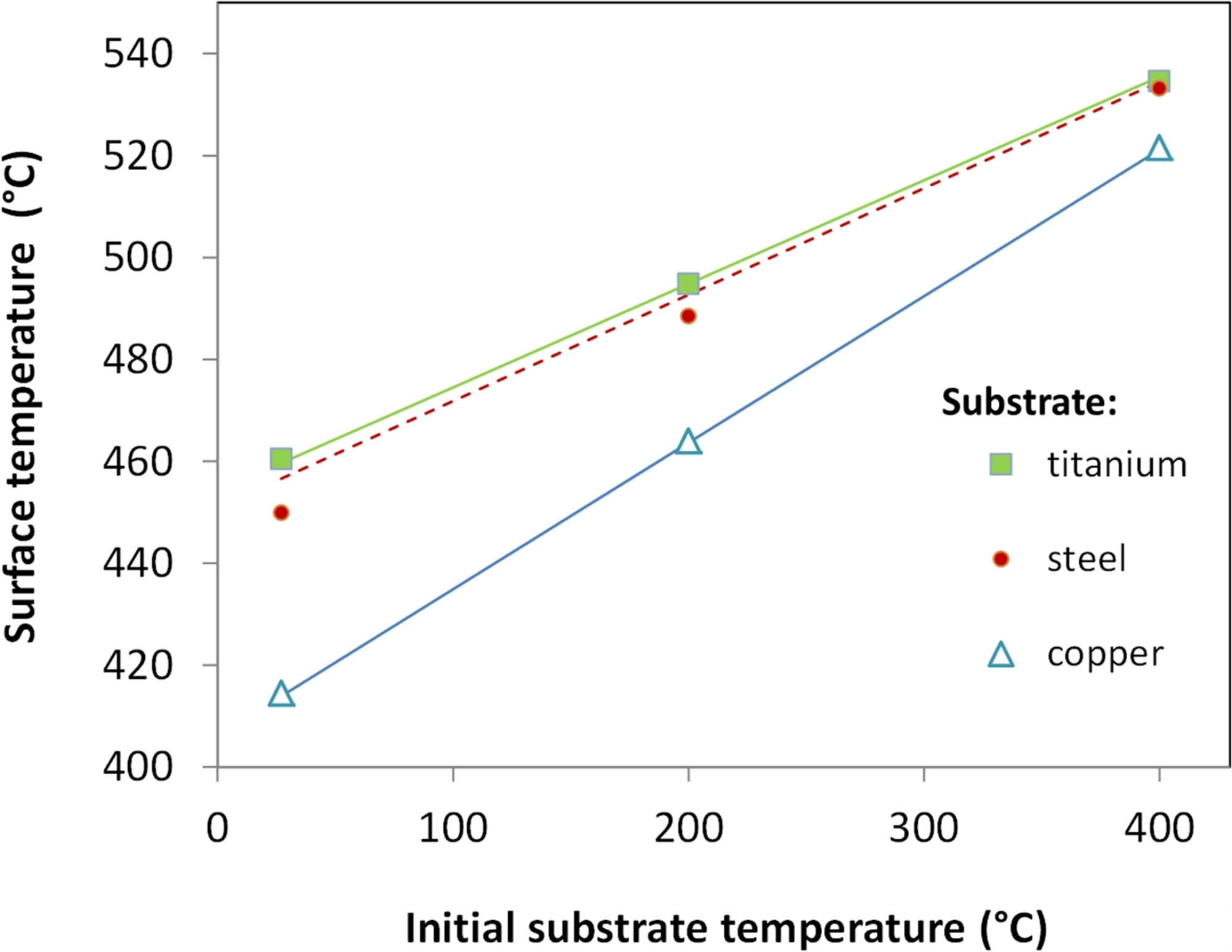
Surface temperature (°C)
540
520
500
480
460
440
420
400
0
100
200
300
400
Initial substrate temperature (°C)
Substrate:
titanium
steel
copper

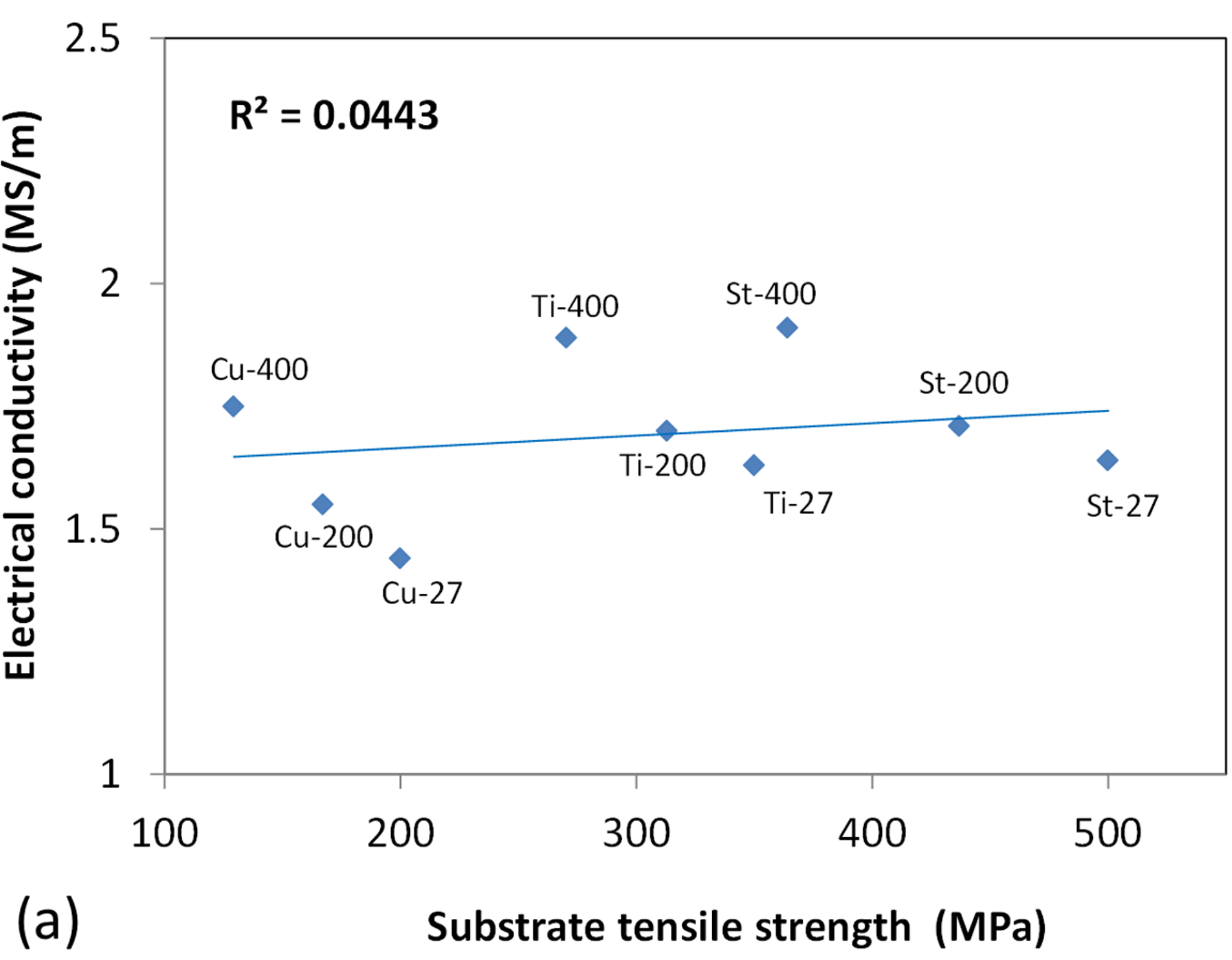
R² = 0.0443
Electrical conductivity (MS/m)
2.5
2
1.5
1
Cu-400
Ti-400
St-400
St-200
Ti-200
Ti-27
St-27
Cu-200
Cu-27
100
200
300
400
500
(a)
Substrate tensile strength (MPa)

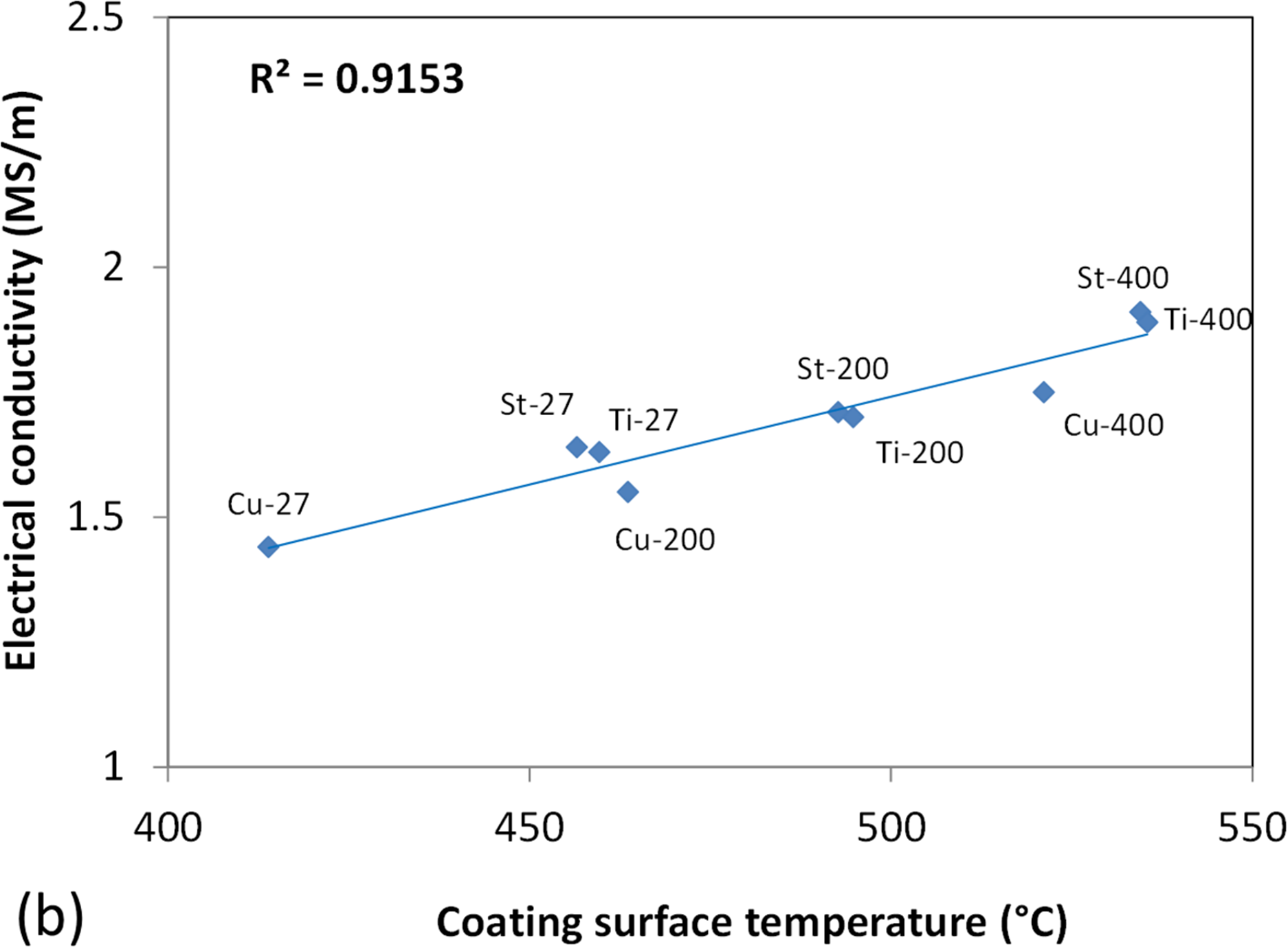
R² = 0.9153
Electrical conductivity (MS/m)
2.5
2
1.5
1
400
450
500
550
St-400
Ti-400
St-200
St-27
Ti-27
Cu-400
Ti-200
Cu-27
Cu-200
(b)
Coating surface temperature (°C)

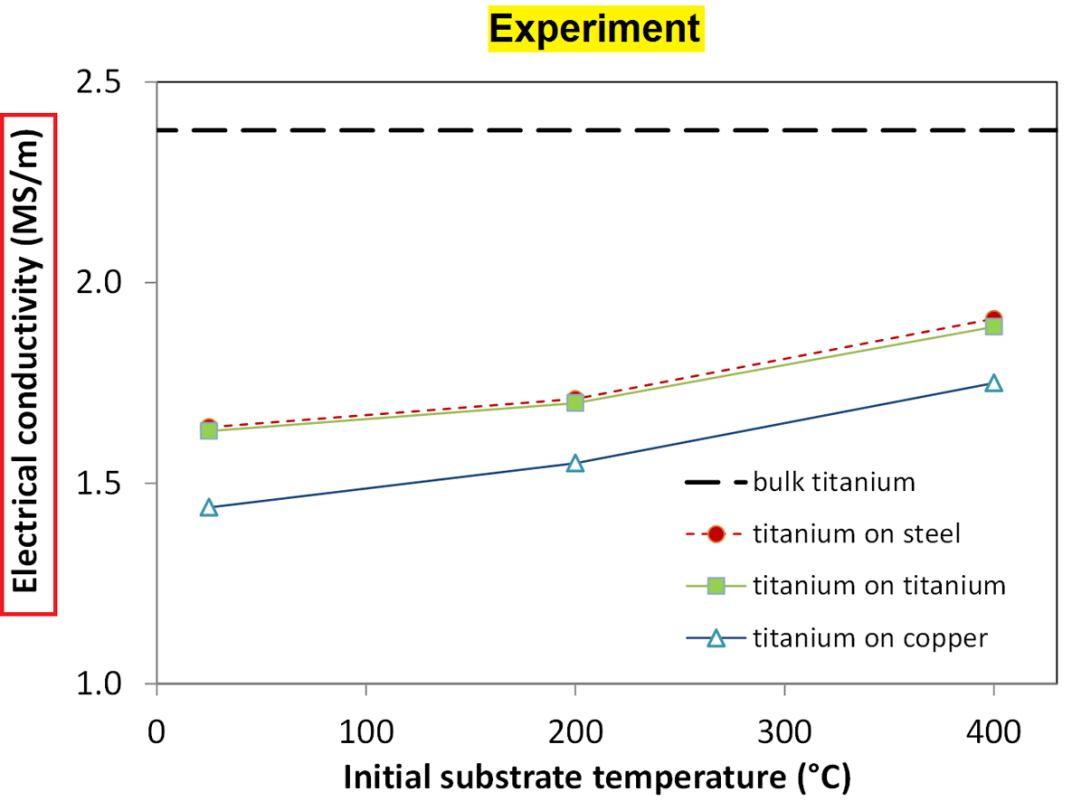
Experiment
Electrical conductivity (MS/m)
2.5
2.0
1.5
1.0
0
100
200
300
400
Initial substrate temperature (°C)
bulk titanium
titanium on steel
titanium on titanium
titanium on copper

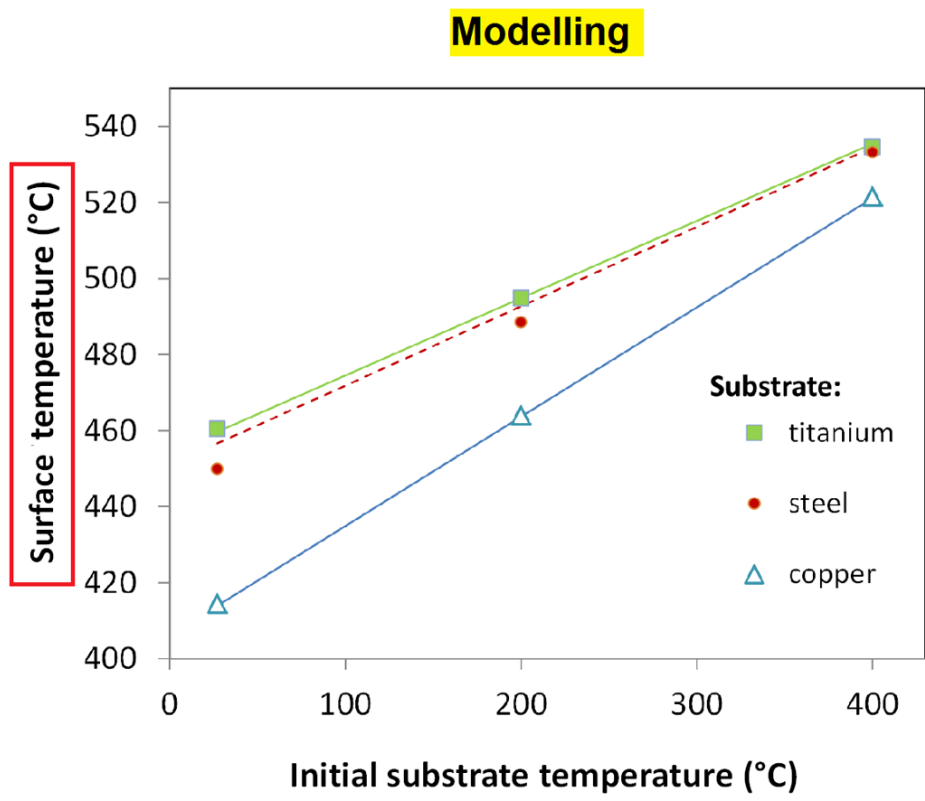
Modelling
Surface temperature (°C)
540
520
500
480
460
440
420
400
0
100
200
300
400
Initial substrate temperature (°C)
Substrate:
titanium
steel
copper